

Lithium mineralizations of Barroso-Alvão aplite-pegmatite field

Filipa Catarina Lopes Dias

Mestrado em Geologia

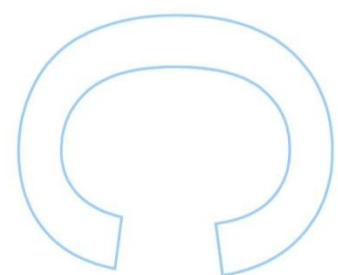
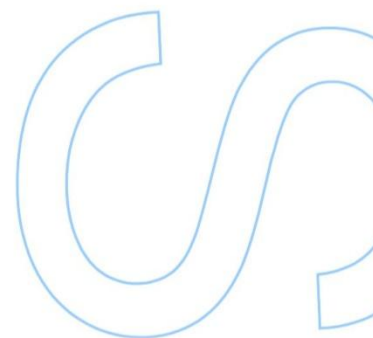
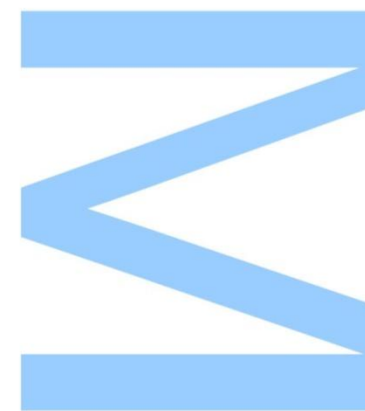
Departamento de Geociências, Ambiente e Ordenamento do Território
2016

Orientador

Alexandre Martins Campos de Lima, Professor Auxiliar, Faculdade de Ciências da Universidade do Porto

Coorientador

Fernando Manuel Pereira de Noronha, Professor Jubilado, Faculdade de Ciências da Universidade do Porto





Todas as correções determinadas
pelo júri, e só essas, foram efetuadas.
O Presidente do Júri,

Porto, ____/____/____

N

S

O

Agradecimentos

Gostaria de apresentar os meus profundos agradecimentos a todas as pessoas que contribuíram para que esta tese se tornasse uma realidade:

Ao professor Alexandre Lima, pela paciência com que sempre ouviu as ideias e teorias que lhe eram propostas.

Ao professor Fernando Noronha que muito me ajudou na compreensão e interpretação das observações feitas no trabalho de campo e na análise petrográfica.

À professora Lia Duarte pela disponibilidade e simpatia com que me ajudou a utilizar o software ArcGis.

À Professora Mona-Liza Sirbescu, da University Central de Michigan, pela ajuda na compreensão e interpretação do que observei no campo.

À Sra. D.^a Irene Lopes por ter sempre tentado ir ao encontro dos pedidos feitos, permitindo-me obter muitos dos dados que são referidos nesta tese.

À Cátia Dias que, como minha colega na área dos pegmatitos, me acompanhou durante a análise de problemas e em saídas de campo.

À Diana Silva por me ter dado coragem e ajudar-me quando precisei.

Aos meus pais e irmã, por me terem apoiado ao longo do decorrer desta tese, em especial ao meu pai que perdeu muito tempo comigo.

Ao meu namorado e melhores amigas que sempre me apoiaram e encorajaram a seguir em frente, com uma referência especial ao primeiro, que acompanhou esta tese do início ao fim.

A todos aqueles que, embora não mencionados especificamente neste local, de alguma forma contribuíram para a conclusão deste trabalho.

Acknowledgments

I would like to express my deepest thanks to all the people who contributed to making this thesis a reality:

To Professor Alexandre Lima for the patience with which he always listened to the ideas and theories that were proposed to him.

To Professor Fernando Noronha who helped me a lot in the understanding and interpretation of the observations that I made in the fieldwork and during the petrographic analysis.

To Professor Lia Duarte for her availability and for the friendliness with which she helped me to use ArcGis software.

To Professor Mona-Liza Sirbescu of the Central Michigan University, for the way she helped me understand and interpret correctly what I observed in the fieldwork.

To Mrs. Irene Lopes for always trying to meet the requests we made, allowing me to obtain many of the data that are referred to in this thesis.

To Cátia Dias who, as my colleague in the pegmatites theme, accompanied me during the analysis of various problems and in all field trips.

To Diana Silva for giving me courage and helping me when I needed it.

To my parents and sister, for having supported me during the course of this thesis, especially to my father who spent a lot of time helping me.

To my boyfriend and best friends who always supported and encouraged me to move on. With a special reference to the first, who accompanied this thesis from the start to the end.

To all those who, although not specifically mentioned at this place, have somehow contributed to the completion of this work.

Abstract

The use of lithium has been increasing over the years. According to the European Commission report of 2014 about the EU critical raw materials, Portugal was the only significant Li producer of the EU, contributing with 0.5% of world production from 2010 to 2014, using only the lepidolite mineral. However, there are three Li-rich regions with spodumene and petalite that have a high potential to be explored and that could also be an important contribution at European level: Serra de Arga, Barroso-Alvão and Almendra-Barca de Alva.

The Barroso-Alvão Li-rich aplite-pegmatite veins are the center of this study. However, countless aplite-pegmatite veins are known in this area and only some of this, hosted in the metasediments of certain lithostratigraphic units, can contain Li-mineralizations.

Therefore, in order to quickly find the Li-rich ones, were created, through ArcGIS software, catchment basins to which were assigned the Li-contents of stream sediments obtained in previous studies of the aplite-pegmatite field of Barroso-Alvão. The created basins have less than 2km², and display the Li-contents analyzed from the stream sediments of 654 sampling points. This way it was created a probability map, with Li-rich areas. It was also possible to define among the Li-rich areas, areas with higher probability of containing petalite aplite-pegmatite veins, through the assignment of Sn-contents to the catchment basins, using the known relation of petalite with cassiterite.

During the field work done in this area, 12 Li-rich aplite-pegmatite veins were observed, as well as, 4 others that are now old Sn mining works. Of the 12 Li-rich veins, 6 were first identified, as having Li-mineralizations, in the course of this thesis.

Most of the aplite-pegmatite veins studied in this work are petalite subtype, despite de fact of existing also spodumene ones, and a large portion of the first has later spodumene (SQI - Spodumene Quartz Intergrowth). In order to better understand this aplite-pegmatite veins that contain both petalite and spodumene, and where the spodumene can be a petalite replacement, there were also made some petrographic studies.

Resumo

O uso do lítio tem vindo a aumentar ao longo dos anos. Segundo um relatório da Comissão Europeia de 2014 sobre os materiais críticos para a UE, Portugal era o único produtor significativo de Li da UE, tendo contribuído com 0.5% da produção mundial entre 2010 e 2014, usando apenas o mineral lepidolite. No entanto, existem três regiões ricas em Li, com espodumena e petalite, com um alto potencial para serem exploradas e que também poderiam ser importantes contribuidores a nível europeu: Serra de Arga, Barroso-Alvão e Almendra-Barca de Alva.

Os filões aplito-pegmatíticos ricos em Li do Barroso-Alvão são o centro deste estudo. No entanto, são reconhecidos numerosos filões aplito-pegmatíticos nesta área e apenas alguns dos filões aplito-pegmatíticos, encaixados em metassedimentos de certas unidades litoestratigráficas, podem conter mineralizações litiníferas.

De modo a encontrar mais rapidamente os filões mineralizados em Li, criaram-se, através do software ArcGIS, bacias de drenagem às quais foram atribuídos os teores de Li de sedimentos de corrente, obtidos em estudos anteriores, do campo aplito-pegmatítico do Barroso-Alvão. Deste modo criaram-se áreas inferiores a 2km² com os teores de Li constatados nos sedimentos de corrente dos 654 pontos de amostragem, obtendo-se assim um mapa de probabilidades de áreas ricas em Li. Também foi possível definir entre as áreas ricas em Li, áreas com maior probabilidade de conter filões aplito-pegmatíticos de petalite, através da atribuição de teores de Sn às bacias de drenagem, usando a relação, já conhecida, da petalite com a cassiterite.

Durante o trabalho de campo feito neste local, observaram-se 12 filões aplito-pegmatíticos mineralizados em Li e 4 outros que correspondem a antigas explorações de Sn. Dos 12 filões mineralizados em Li, 6 foram identificados, como mineralizados em Li, pela primeira vez, no decorrer desta tese.

A maioria dos filões aplito-pegmatíticos estudados são de petalite, apesar de também existirem de espodumena, e uma grande parte dos primeiros possui espodumena posterior à petalite (SQI – Spodumene Quartz Intergrowth). De forma a melhor entender os filões aplito-pegmatíticos que

contém tanto petalite, como espodumena, e onde a espodumena pode substituir a petalite, fizeram-se também alguns estudos petrográficos.

Keywords

Pegmatites, Li, spodumene, petalite, ArcGIS

Palavras-chave

Pegmatitos, lítio, espodumena, petalite, ArcGIS

Table of Contents

Agradecimentos	v
Acknowledgments	vi
Abstract	vii
Resumo	viii
List of Figures	xiv
List of Tables	xviii
List of abbreviations	xix
Chapter 1 – Introduction	21
Chapter 2 – Geological Setting	27
Chapter 3 – Desk work with ArcGIS software	37
Chapter 4 – Field work and sampling	45
4.1. N312-1 and N312-2 aplite-pegmatite veins	51
4.2. CHN3 aplite-pegmatite vein	53
4.3. Alijó aplite-pegmatite vein	55
4.4. Pinheiro aplite-pegmatite vein	58
4.5. Vila Grande aplite-pegmatite vein	59
4.6. Lousas aplite-pegmatite vein	60
4.7. AL56 aplite-pegmatite vein	63
4.8. Gondiaes aplite-pegmatite vein	65
4.9. Dias 1 aplite-pegmatite vein	66
4.10. Dias 2 aplite-pegmatite vein	66
4.11. Dias 3 aplite-pegmatite vein	67
Chapter 5 – Petrographic and mineralogical study	69
5.1. AL56	71

5.2. CHN3	74
Chapter 6 – Discussion and conclusions	79
References	83
List of websites consulted	88
Annexes	91
Annex 1	93
Annex 2	94

List of Figures

Fig. 1- Lithium world production, in tonnes, from 2010 to 2014. The trend line as a positive slope. (Reichl <i>et al.</i> , 2016).....	23
Fig. 2 – Lithium world production from 2010 to 2014 (Reichl <i>et al.</i> , 2016)	24
Fig. 3 - Geologic map of the study area located in Barroso-Alvão aplite-pegmatite field. Most of the known Li-rich aplite-pegmatite veins are located in Sb and SCunits. Adapted from “Mapa Geológico de la Península Ibérica, Baleares y Canarias`” scale 1:1 000 000, 2015 edition. Available in IGME (Instituto Geológico y Minero de España) website, 26 Jan. 2016. This geological map was created by IGME and LNEG (Laboratório Nacional de Energia e Geologia) (Portugal).	29
Fig. 4- Gondwana and Rheic oceans. Adapted from “Key time slices in North American History” from “Library of Paleogeography”, Colorado Plateau Geosystems, Inc website, retrieved: 15/02/2016	30
Fig. 5 – Lithostratigraphic units of TMSD (Ribeiro, 1999)	31
Fig. 6 - Lithostratigraphic units of CSD (Ribeiro, 1999).....	32
Fig. 7- PT diagram of spodumene, eucryptite and petalite stability fields. Adapted from: fig. 7-7, pag. 116, book “Pegmatites” of David London, 2008, Mineralogical Association Canada.....	34
Fig. 8 - Schematic representation of the P-T fields of the pegmatites host rock, where you can observe the following classes: abyssal (AB), muscovite (MS), rare muscovite elements (MSREL), rare elements (REL) and miarolitic (MI). Arrows indicate regional fractionation trends present in pegmatites in relation to metamorphic gradients of the wall rocks. In some cases there are passages of a class to another, such as in cases of MS classes and MSREL, and in the cases of classes REL and MI (figure obtained from Cerny and Ercit 2005).....	35
Fig. 9 - (A) Satellite image of the study area retrieved from the “World Imagery” map service of ArcGIS v. 10.3. (B) Representation of the flow direction image within the study area (“clip_flow”).....	40
Fig. 10 – Representation of the “flow_accum” raster-based file that resulted from the “Flow Accumulation” tool. The black pixels represent the 0-70 class and white pixels represent the 70-479464 class, allowing the view of the waterlines. The red points represent the “SS” points.	40

Fig. 11 – Representation of “SetNull” raster-based file that resulted from the “Set Null” tool. The black pixels have a value of 1 and represent the waterlines within the study area.....	41
Fig. 12 – Representation of the catchment basins raster image (“bacias_raster”) resultant from the Watershed tool. Each color represents one catchment basin that was created from a “SS” point and from the “clip_flow” raster image, that provided the information about the flow direction according to the terrain topography.	41
Fig. 13- Conversion errors from the raster image to the shapefile. (A) Representation of the catchment basins raster-based file. (B) Representation of the result of the conversion to a shapefile with the resulting subdivision of some catchment basin polygons into small individual ones. (C) Representation of the new and corrected catchment basins shapefile.	42
Fig. 14 – Representation of “Bacia_dreno_final” file, where each color represents a different class of Li contents.....	43
Fig. 15 - Locations of the 12 Li-mineralized veins observed in the field, together with the representation of the Li-bearing catchment basins, as well as the mining concessions that can be found here.	49
Fig. 16 - Locations of the 12 Li-mineralized veins observed in the field, together with the representation of the Sn-bearing catchment basins, as well as the mining concessions that can be found here.	50
Fig. 17 – (A) Legend with the symbols, structures and lithostratigraphic units from the geological maps shown in fig. 15 and Fig. 16, corresponding to sheet 6C - Cabeceiras de Basto, scale 1: 50000. (B) Li- and Sn-content classes used in the representation of the catchment basins from fig. 15 and fig. 16.	50
Fig. 18 – Feldspar crystals growing in a comb structure from the aplite-pegmatite (N312-2) contact with the country rock.....	51
Fig. 19 – Localization of N312-1 and N312-2 aplite-pegmatite veins on the Li-bearing (fig. 19A) and Sn-bearing (fig. 19B) catchment basins maps, using 6D - Vila Pouca de Aguiar sheet of the Geological Map of Portugal. The blue lines represent the waterlines.	52
Fig. 20 – Petalite crystal from CHN3 aplite-pegmatite vein.....	53
Fig. 21 - Two shear-zones cross-cutting the aplite-pegmatite vein: a shear-zone with attitude N132 °; SV and a later one with attitude N160 °; SV. Both are right-lateral (indicated by the yellow arrows).....	54

Fig. 22 - (A) Small shear-zone filled by quartz and with spodumene in the edges, observed in CHN3 aplite-pegmatite vein. (B) Close-up of the shear-zone represented in fig. 22A.....	54
Fig. 23 – Alijó aplite-pegmatite vein exploration site. (A) Exploration site photo. (B) Satellite image of the exploration site. Google Earth adapted image. (C) Schematic figure representative of the contacts directions observed in the exploration site of the aplite-pegmatite vein and of a shear plane located north of the exploration.....	55
Fig. 24 – D3 shear corridor at the exploration site of Alijó aplite-pegmatite vein.....	56
Fig. 25 – (A) Collected sample with several spodumene crystals. (B) Close-up of fig. 25.A.....	57
Fig. 26 - Pinheiro aplite-pegmatite vein. (A) Satellite image with the representation of the structural setting observed during field work. This image was adapted using the ArcGIS 10.3 World Imagery service. (B) Spodumene crystal.....	58
Fig. 27 - Location of Pinheiro aplite-pegmatite vein on the Li-bearing (fig.27A) and Sn-bearing (fig.27B) catchment basin maps, using the 6C - Cabeceiras de Basto sheet, from the Geological Map of Portugal. The blue lines and blue points represent the waterlines and “SS” points respectively.....	58
Fig. 28 - (A) Columbo-tantalite and petalite from Vila Grande aplite-pegmatite vein. (B) Close-up of the columbo-tantalite crystal from fig. 28A.	59
Fig. 29 - Vila Grande aplite-pegmatite vein location on the Li-bearing (fig. 29A) and Sn-bearing (fig.29B) catchment basin maps, using 6C - Cabeceiras de Basto sheet, from the Geological Map of Portugal. The blue lines and blue points represent the waterlines and “SS” points respectively.	59
Fig. 30 - Spodumene with quartz intergrowths (SQI - Spodumene Quartz Intergrowth)	60
Fig. 31 - Petalite crystals randomly distributed in Lousas aplite-pegmatite vein. In these crystals can be seen very well the translucent appearance of fresh petalite.....	61
Fig. 32 – Location of Lousas aplite-pegmatite vein on the Li-bearing (fig. 28A) and Sn-bearing (fig.28B) catchment basin maps, using 6C - Cabeceiras de Basto sheet, from the Geological Map of Portugal. The blue lines and blue points represent the waterlines and “SS” points respectively.	61
Fig. 33 - Direction of the pegmatitic melt and petalite crystals fragments of Lousas aplite-pegmatite vein. The arrows indicate the fluid	

direction and the black dashed lines represents the crystallization fronts. The red dashed line outline the petalite broken crystals area, being that they are the darker ones...... 62

Fig. 34 - Deformed feldspars from the aplite-pegmatite vein located in the AL56 vein area. 63

Fig. 35 – Sample with SQI crystals from the aplite-pegmatite vein located in the AL56 vein area. 63

Fig. 36 - Location of the aplite-pegmatite vein present in the AL56 vein area in the Li-bearing (fig.36A) and Sn-bearing (fig.36B) catchment basin maps, using the 6C - Cabeceiras de Basto sheet, from the Geological Map of Portugal. 64

Fig. 37 - Gondiães aplite-pegmatite vein location on Li-bearing (fig. 36A) and Sn-bearing (fig. 36B) catchment basin maps, using 6C - Cabeceiras de Basto sheet, from the Geological Map of Portugal. 65

Fig. 38 – Petalite crystals from Dias 1 aplite-pegmatite vein sample. ... 66

Fig. 39 – Dias 3 aplite-pegmatite vein location on the Li-bearing (fig. 39A) and Sn-bearing (Fig. 39B) catchment basin maps, using the 6D - Vila Pouca de Aguiar sheet, from the Geological Map of Portugal. 67

Fig. 40 - Aplite-pegmatite vein sample from AL56 aplite-pegmatite vein area, where it can be seen with the naked eye, a petalite crystal being replaced by spodumene + quartz (SQI). This sample also contains other petalite crystals. 71

Fig. 41 - Thin section photomicrograph from the sample referred above (fig. 40) where a petalite crystal is being replaced by spodumene + quartz (inside the red dashed line), next to another petalite crystal (on the right side). (A) Plane polarized light. (B) Cross polarized light. 71

Fig. 42 – Photomicrograph of some of the spodumene aspects from aplite-pegmatite vein in the area of AL56 vein. (A) Lateral replacement of petalite by spodumene and quartz. (B) SQI replacement in another petalite crystal, where the spodumene + quartz resemble a symplectite texture. (C) Close-up on the spodumene and quartz within the main petalite crystal from figure 40 and figure 41. 73

Fig. 43 – Shear corridor from CHN3 aplite-pegmatite vein, with ultramylonitic to mylonitic texture, where most of the ocelli indicate that this is a dextral shear. (B) Ocelli in plane polarized light. (C) Ocelli in cross polarized light. The yellow arrows show the ocelli indicating that this is a dextral shear. . 74

Fig. 44 - Photomicrograph of petalite being replaced by spodumene and quartz (SQI) from CHN3 aplite-pegmatite vein..... 76

Fig. 45– Photomicrograph of some features of spodumene from CHN3 aplite-pegmatite vein. (A) Largest spodumene and quartz crystals in an elongated aggregate, where it's possible to see the symplectite texture at one end. (B) Close-up of fig. 41A. (C) Small spodumene and quartz crystals in an elongated aggregate. (D) Close-up of Fig. 41C. (E) Small spodumene crystals posterior to the shear..... 77

Fig. 46 – Photomicrograph with some features of the CHN3 thin section. (A) Ambligonite ocelli with pressure shadows. (B) Albites with deformation induced twinning and bent twinning. (C) Vermicular quartz inclusions on an albite crystal. (D) Small crystals of quartz and albite forming what seems to be a mosaic. (E) Quartz resulting from dynamic recrystallization. (F) Deformed moscovite. (G) Microcline with the typical cross-hatched twin pattern (H) Fractured cassiterite. (I) Deformed cassiterite within a shear corridor. (J) Apatite inclusion on quartz..... 78

Fig. 47 – Location of Romano old Sn mine (green point) in the Li-bearing (fig.47A) and Sn-bearing (fig.47B) catchment basin maps. The coordinates of this aplite-pegmatite vein are 41°44'14.592" W7° 43'43.591"W. The red outline represents the planned drill area by Dakota Minerals. In Pires (2005) this zone had already been identified as having high Li-contents, as represented by the black counter lines in the fig.47A. The catchment basins create now smaller and more precise Li-rich areas. 81

List of Tables

Table 1 – Some examples of brine deposits with Li concentrations (ppm) (Moura and Velho, 2011).....22

List of abbreviations

Ppm – Parts per million

UE – European Union

LNEG – Laboratório Nacional de Energia e Geologia

GTMZ – Galicia Trás-os-Montes Zone

CIZ – Central Iberian Zone

CSD – Carracedo Structural Domain

TMSD – Três Minas Structural Domain

SV – Subvertical

SH – Subhorizontal

Pet – Petalite

Qtz – Quartz

Spd – Spodumene

SQI - Spodumene Quartz Intergrowth

SS – Stream sediments

FD – Flow Direction

D₁, – First phase of deformation of Variscan Orogeny

D₂ – Second phase of deformation of Variscan Orogeny

D₃ – Third phase of deformation of Variscan Orogeny

S₁ – Main foliation resulting from D₁

S₂ - Main foliation resulting from D₂

S₃ - Main foliation resulting from D₃

Chapter 1 – Introduction

Nowadays, lithium (Li) is mainly used in the ceramics and glass industries, but its use has been increasing due to the manufacture of rechargeable batteries, used, for example, in portable electronic equipment (European Commission, 2014).

During the geological evolution of the earth's crust, sometimes "traps" are formed, allowing the concentration of some chemical elements. These "traps" tend to exceed the average abundance of these elements in the Earth's crust.

Lithium abundance in Earth's crust is 20 ppm. However, quantities economically exploitable can be found both in pegmatites and in brine deposits. The later have volcanic contribution and the lithium is concentrated through solar evaporation.

Obtaining Li through the brine deposits become less expensive than the metallurgical processing required when exploiting pegmatites. However, if in the coming years the consumption of lithium increases, as expected, the pegmatites will be more valued since they are an important source of lithium (European Commission, 2014a; Moura and Velho, 2011).

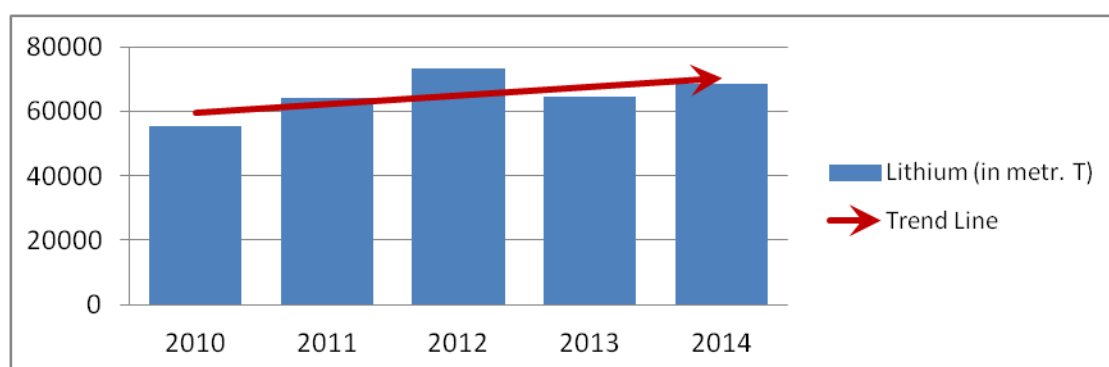


Fig. 1- Lithium world production, in tonnes, from 2010 to 2014. The trend line as a positive slope. (Reichl et al., 2016)

The use of lithium has been increasing in the automotive industry, for which the technology of choice used in the electric and hybrid vehicles batteries is the lithium ion. As this type of vehicle is, at this moment, a world bet, there are those who already consider it the gasoline of the future.

In 2014, a report of critical raw materials for the European Union (EU) indicated that the main uses of lithium were 30% in the industries of ceramics and glass and 22% in electric batteries.

The EU is a major importer of Li, and imports about 13,000t per year of Li carbonate and Li oxides and hydroxides. Most of this is imported from Chile (European Commission, 2014a).

Brine deposits have become the main mineral resource of lithium and the largest reserves in the world are located precisely in Chile, which has half of world reserves, not to mention the other countries of South America that also have significant reserves.

According to the report on critical materials for the European Union in 2014, the United States Geological Survey (USGS) said that the world reserves of lithium are about 40 million tons (European Commission, 2014a).

Table 1 – Some examples of brine deposits with Li concentrations (ppm) (Moura and Velho, 2011)

South America	Chile	1000 - 5000 ppm
	Argentina	100 - 700 ppm
	Bolivia	100 - 500 ppm
Asia	Tibet	700 - 1000 ppm
	China	100 ppm
North America	Nevada (EUA)	100 - 300 ppm

In recent years (from 2010-2014), Chile and Australia have been the main producers of Li. In this period they produced, respectively, 39% and 33% of world production (126,070t and 107,713t) (Reichl *et al.*, 2016).

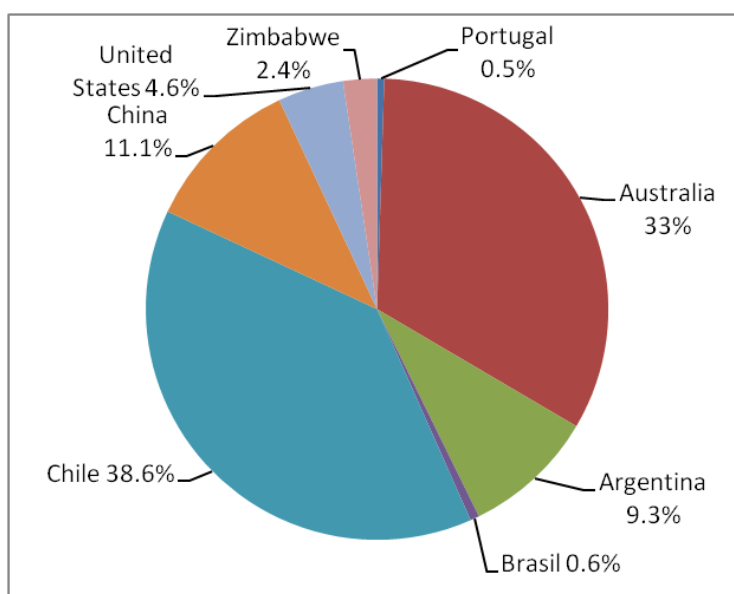


Fig. 2 – Lithium world production from 2010 to 2014 (Reichl *et al.*, 2016)

The Australian reserves consist in pegmatites only, being that its largest mineral deposits are from spodumene. The Li contribution made by Zimbabwe is also derived from pegmatites, but from the petalite mineral (European Commission, 2014th, Australian atlas of minerals resources, mines & processing centers, 2013; Sitando and Crouse, 2011).

According to European Commission (2014) and Reichl *et al.* (2016), until 2014, Portugal was the only EU country with significant reserves of lithium that has been contributing to the world production, through the lepidolite mineral of aplite-pegmatite origin from Goncalo-Vela area (Guarda district). This area has been indicated as having the highest gross reserves of Li in Portugal. According to Moura and Velho (2011), Ramos (2000) assessed them as being more than 1 400 000t.

From 2010 to 2014, Portugal has contributed to the lithium world production with 1 615t (Moura and Velho, 2011; European Commission, 2014, Reichl *et al.*, 2016).

The minerals considered more important for obtaining Li are spodumene ($\text{LiAlSi}_2\text{O}_6$), lepidolite ($(\text{K}_2(\text{Li},\text{Al})_{5-6}(\text{Si}_{6-7}\text{Al}_{2-1}\text{O}_{20})(\text{OH},\text{F})_4$), amblygonite ($(\text{LiAl}(\text{PO}_4)(\text{F},\text{OH}))$) and Petalite ($\text{LiAlSi}_4\text{O}_{10}$), corresponding to them, theoretically, 3.7% Li, 3.6% Li, 4.7% Li, 2.3% Li, respectively. However, due to substitutions which generally occur between different elements, spodumene content ranges from 1.3% - 3.6%, the lepidolite content between 1.4% - 1.9%, the amblygonite content between 3.5% - 4.2% and the contents of petalite between 1.6% - 2.1% (European Commission, 2014; Moura and Velho, 2011; Kogel *et al.*, 2006).

According to the report on critical materials for the European Union in 2014, the United States Geological Survey (USGS) reported the existence of two lithium related mining projects, namely, a spodumene exploration project in Finland and a jadarite mining operation in Serbia, which is a candidate country to the European Union.

The mineral jadarite ($\text{LiNaB}_3\text{SiO}_7(\text{OH})$) is a new species recently discovered in Serbia, to which was assigned theoretically a 3.4% Li-content (Bryner *et al.*, 2013).

Despite the fact of the European Commission (2014) stating that the Portuguese significant amount of lithium production is derived from the lepidolite mineral, there are three Li-rich regions with spodumene and petalite that have a high potential to be explored and that could also be an important contribution at an european level: Serra de Arga, Barroso-Alvão and Almendra-Barca de Alva (Viegas *et al.*, 2012; European Commission, 2014).

The Li-rich aplite-pegmatite veins of Barroso-Alvão are the center of this study. Some of the studied aplite-pegmatite veins were already known to be Li-mineralized, but in other veins these mineralizations weren't identified until the development of this study. For example, Alijó aplite-pegmatite vein, in which the main lithium mineral is spodumene, were already appraised 402,800t of ore with an average grade of 1.40% of Li_2O (0.65% Li, or 6500ppm) (Moura and Velho, 2011).

The aplite-pegmatite field of Barroso-Alvão has a lot of aplite-pegmatite veins, some of which have been explored in the past to obtain Sn. Currently the only lithium veins explorations are for the ceramics and glass industries.

The lithium concentrations within mining concessions with aplite-pegmatite veins, that have a lot of spodumene and petalite with high Li-contents, should also be seen as a potential source of Li-carbonate for the chemical industry. Meanwhile, the veins with petalite should be considered better for the ceramics and glass industries since they usually have a low content of iron and other contaminants (Lima et al, 2011).

The lithium potential of the aplite-pegmatite field Barroso-Alvão was first discovered in 1987, during a petrographic study of granites and the elaboration of the geological mapping of 6C sheet (Cabeceiras de Basto), scale 1: 50000, of the Geological Map of Portugal.

The team of Professor Fernando Noronha, during the preparation of the four geological maps covering this area at 1: 50000 scale (6-A, Montalegre, 6-B, Chaves; 6-C, Cabeceiras de Basto, 6-D, Vila Pouca de Aguiar) charted a lot of aplite-pegmatite veins, including veins with spodumene, which were the first lithium mineralized veins to be described.

At this time, it was also taken into account the pegmatites with lepidolite and phosphates of the amblygonite-montebrazite series and aplites associated with tin mineralizations, as well as the host rocks and their tectonic setting.

Many of the aplite-pegmatite veins observed in the Barroso-Alvão aplite-pegmatite field were exploited to obtain cassiterite as tin ore, but most of the methods used for its exploration were artisanal causing the choice of the most friable ones.

In 2003, under the guidance of Professor Alexandre Lima, it was discovered aplite-pegmatite veins in which petalite was the dominant phase, when compared to spodumene.

Because of the importance of these mineralizations, there have been several studies at the mineralogical, petrological, and geochemical levels, spatial analysis and in the exploration context, such as Charoy and Noronha (1988) Dória *et al.* (1989) Noronha e Charoy (1991), Charoy *et al.* (1992); Pires (1995), Amarante *et al.* (1999), Farinha and Lima (2000), Lima (2000), Charoy *et al.* (2001), Martins (2009), Martins and Lima (2011) and Silva (2014).

Chapter 2 – Geological Setting

The Barroso-Alvão aplite-pegmatite field is located in the Trás-os-Montes region, North of Portugal. From the geotectonic point of view, it is located in the Northwest of the Hesperic Massif, in the parautochthonous metasedimentary sequences of the "Galicia Trás-os-Montes Zone" (GTMZ), more precisely, to the west of Régua-Verín fault.

As indicated in geological cartography the host-rocks of the Li-rich aplite-pegmatite veins are metasedimentary sequences of early Paleozoic (late Ordovician to Devonian), with low to medium grade metamorphism.

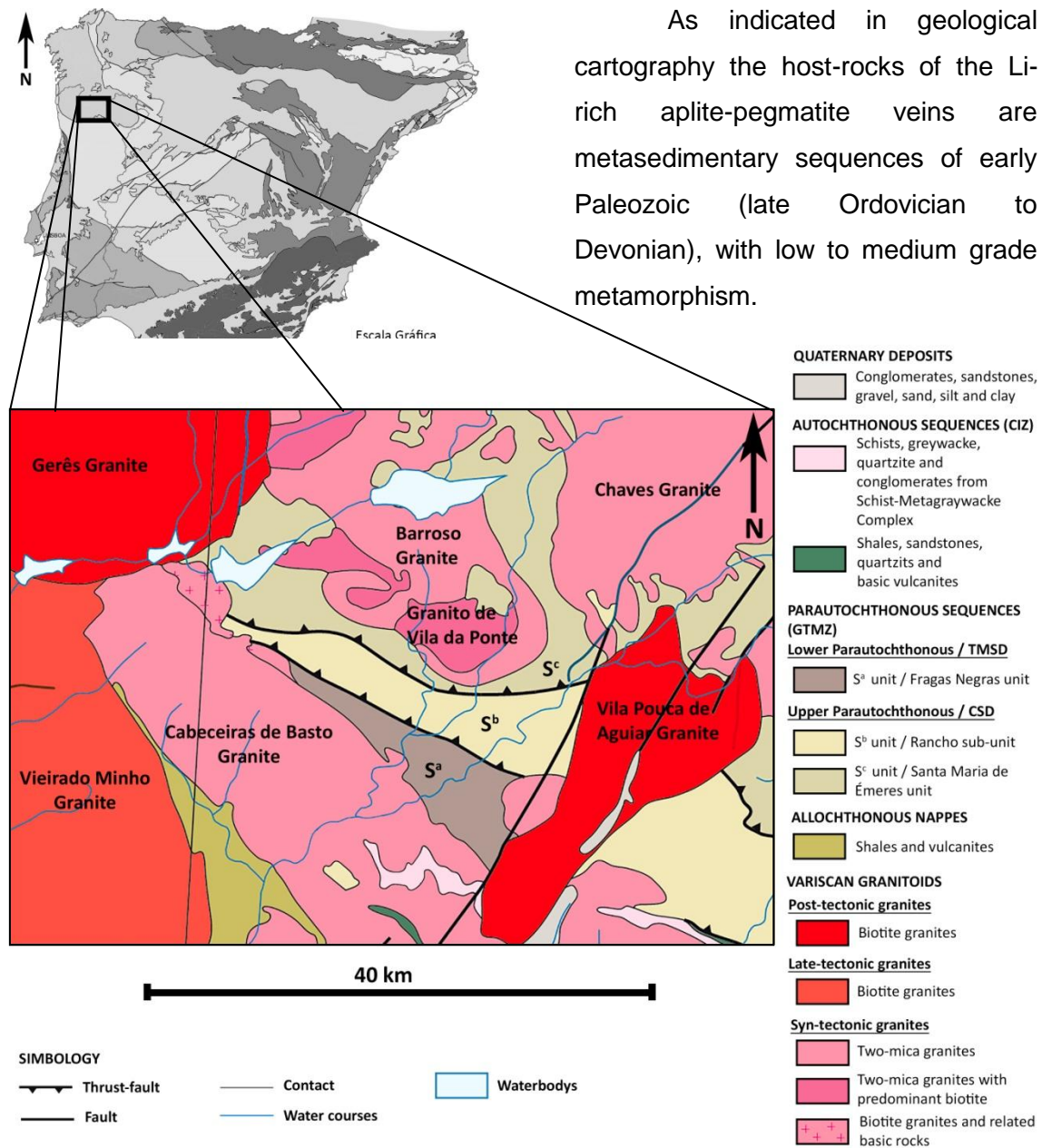


Fig. 3 - Geologic map of the study area located in Barroso-Alvão aplite-pegmatite field. Most of the known Li-rich aplite-pegmatite veins are located in S^b and S^c units. Adapted from "Mapa Geológico de la Península Ibérica, Baleares y Canarias" scale 1:1 000 000, 2015 edition. Available in IGME (Instituto Geológico y Minero de España) website, 26 Jan. 2016. This geological map was created by IGME and LNEG (Laboratório Nacional de Energia e Geologia) (Portugal). ([http://info.igme.es/cartografiadigital/datos/geologicos1M/Geologico1000_\(2015\)/pdfs/EditadoG1000_\(2015\).pdf](http://info.igme.es/cartografiadigital/datos/geologicos1M/Geologico1000_(2015)/pdfs/EditadoG1000_(2015).pdf))

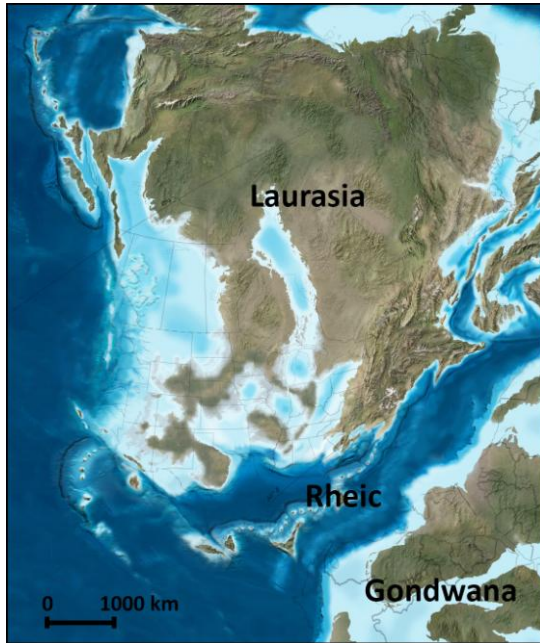


Fig. 4- Gondwana and Rheic oceans. Adapted from "Key time slices in North American History" from "Library of Paleogeography", Colorado Plateau Geosystems, Inc website, retrieved: 15/02/2016 (http://cpgeosystems.com/images/NAM_key-375Ma.jpg)

The GTMZ tectonic setting is due to the Variscan Orogeny, defined by a succession of three main deformation phases (D_1 , D_2 and D_3). These three phases produced three main foliations in the host-rocks of the aplite-pegmatite veins (S_1 , S_2 , S_3) (Martins, *et al.*, 2006; Sant' Ovaia, *et al.*, 2011).

The Variscan mountain range was the result of the continental collision of Laurasia and Gondwana, closing the Rheic ocean, and creating an overthrust of several structural units (crustal nappes), separated by thrust faults, that built the GTMZ.

The boundary of this zone is marked by a large D_2 thrust fault that places all allochthonous and parautochthonous nappes over the autochthonous sequences (Douro Inferior Domain of CIZ - Central Iberian Zone) (Noronha, *et al.*, 2006).

D_1 phase generated folds with a predominant orientation NW-SE. Parautochthonous units folding has a dipping axial plane and an S_1 foliation that was later reoriented by phase D_2 .

D_2 phase has a continuity in style with D_1 phase, highlighting the SE folding dip, creating overturned folds, with a very short limb. In the parautochthonous units, the D_2 phase forced S_1 foliation to be horizontalized, resulting in a crenulation cleavage (S_2).

D_3 phase is represented by a small amplitude folding, with a vertical axial plane, as well as vertical ductile shear zones. On a regional scale, the parautochthonous units show the results of D_3 phase by folds of subhorizontal hinge and $N100^\circ$ to $N120^\circ$ subvertical axial plane.

Afterwards a period of ductile-brittle and brittle deformation succeeded (late- D_3 and post- D_3) creating a conjugated fractures systems with NNE-SSW and NNW-SSE azimuths, where the first orientation is the more considerable. An example of the NNE-SSW fractures system is the Régua-Verin fault that was nucleated in D_3 phase and

then reactivated as strike-slip fault. In this fault we can see two different crustal levels, a deeper level located to the west of the fault and another one less deep on the east side (Noronha *et al.*, 2006, Ribeiro, 1998; Sant' Ovaia *et al.*, 2011).

GTMZ parautochthonous units are divided in two domains from a lithostratigraphic, lithochemistry and structural point of view, separated by a larger thrust fault (Palheiros-Vila Flor trust fault).

Both these domains have different designations on the 6-C and 6-D sheets of the Geological Map of Portugal, scale 1:50000: in 6-C the lower domain is identified as Lower Parautochthonous, and the upper domain as Upper Parautochthonous, while in 6-D this are identified as Três Minas Structural Domain (TMSD) and Carrazedo Structural Domain (CSD) respectively.

The parautochthonous units of GTMZ, have similar lithostratigraphic characteristics to the autochthonous units of CIZ, being that the DETM units are correlated with autochthonous units of the Lower Douro Domain.

The paleographic interpretation of the Parautochthonous Domain, of GTMZ, indicates deposition in the margin of Gondwana, where the CIZ autochthonous was deposited, from Pre-Cambrian to Devonian. The lithogeochemistry composition of parautochthonous units indicates that initially the sedimental basin was an anoxic environment, suggesting a passive margin (TMSD), and latter became a more oxygen rich environment, active margin (CSD).

The TMSD (fig. 5) consists of two lithostratigraphic units, called Fragas Negras unit (base unit) and Curros unit (top unit), but only the unit of Fragas Black was individualized in aplite-pegmatite field Barroso - Alvão, at west of Régua-Verin fault. This unit is correlative with the autochthonous units of the Marão region, such as the formation of Campanhó, and corresponds to S^a unit in 6-C sheet.

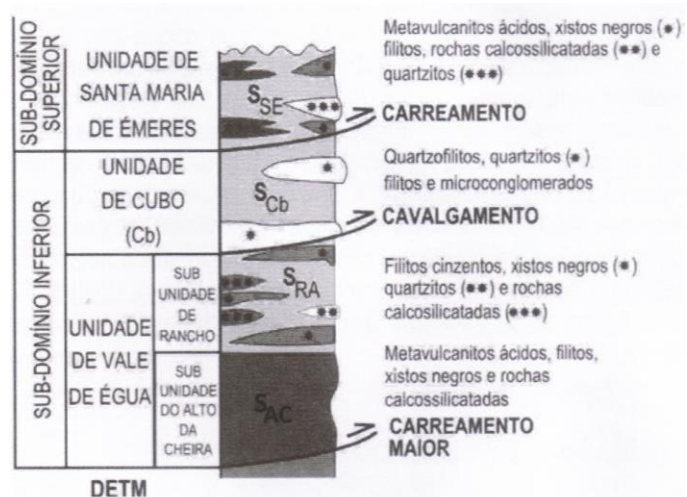


Fig. 5 – Lithostratigraphic units of TMSD (Ribeiro, 1999)

therefore, with the metamorphic processes. Thus, these granites were also marked by a S_3 foliation, NW-SE.

The relation of the metamorphic processes with sintectonic and tardi-tectonic granites in the study area is evident. The granites have an elongated shape, of NW-SE direction, parallel to the regional structure. Also, along Cabeceiras de Basto granite, and at south of Fragas Negras unit it's possible to see regional metamorphism isograds, parallel to the igneous contacts and lithostratigraphic contacts resulting from the thermal peak, late- D_3 to syn- D_3 , derived from a prograd dynamothermal evolution. This evolution is expressed by the occurrence of early staurolite, relative to andalusite, and by the existence of andalusite and cordierite poikilitics, late- to post- tectonic.

According to Lima (2000), data from Holtz (1987) allowed to classify the sintectonic two-mica granites of Cabeceiras de Basto and Barroso as a type of granite strongly differentiated through Bouseily El & El Sokkary (1975) diagram.

The post-tectonic biotite granitoids with calcic plagioclase, occur in massives with an elongated form, that takes advantage of deep fractures, generated at the end of D_3 -phase, to intrude. They are considered as having originated at a deep crustal level, are subalkaline and usually intrude in the upper crust since they are formed by a dry magma that can travel longer distances over the crust. An example of this type of granites is Vila Pouca de Aguiar granite (Sant 'Ovaia *et al.*, 2011; Noronha *et al.*, 2006).

According to a genetic model, created in recent studies, the rare elements-rich pegmatites may result from a low melting rate of crustal material with successive injections of different melts, favored by regional shear-zones, as it seems to happen in Monts d'Ambazac pegmatitic field, Central massif, France and in Forcarei pegmatite field, NW of Galícia, Spain.

Forcarei field southern border is limited by Celanova migmatitic dome, derived from a low temperature hydrated melt, derived from the fusion of crustal material (Deveaud *et al.*, 2014).

Barroso-Alvão aplite-pegmatite field also fits in these examples, showing a spatial association between, granites, migmatites, shear zones and aplite-pegmatite veins, classified according to Cerný and Ercit (2005) as rare elements pegmatites, of the LCT family (Li, Cs, Ta), complex type and petalite and spodumene subtypes.

In Barroso-Alvão aplite-pegmatite field also seems to exist a structure similar to Celanova migmatitic dome, named Barroso-Alvão dome, which is limited in the west by Gerês granite, named Barroso-Alvão dome.

In the area, a large amount of aplite-pegmatite veins seems to be structurally controlled by existing foliations, and D_3 related planes, with an azimuth of $N130^\circ$ and NS to $N10^\circ$, suggesting they were emplaced along the preferential structural planes during and after the peak of metamorphism (Deveaud *et al.*, 2014; Noronha *et al.*, 2006).

According to Noronha *et al.*, (2006) the fact that spodumene veins seem to be posterior to the petalite veins, and the first were formed at lower pressures, suggests an evolution related to an up-lift process.

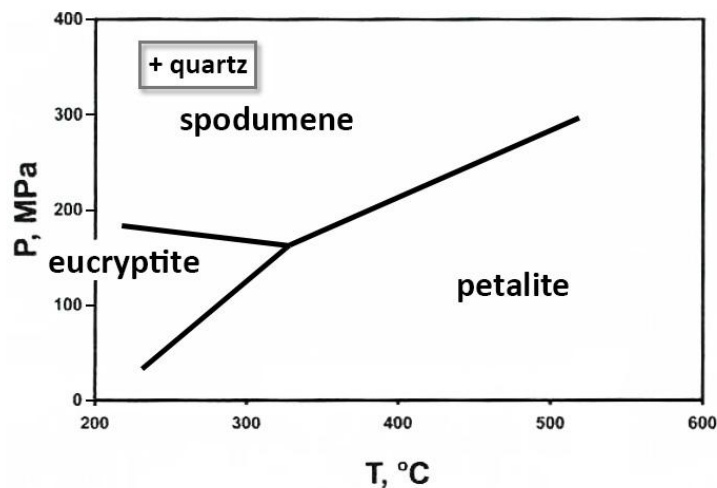


Fig. 7- PT diagram of spodumene, eucryptite and petalite stability fields. Adapted from: fig. 7-7, pag. 116, book "Pegmatites" of David London, 2008, Mineralogical Association Canada

By classifying the pegmatites we are assigning them a set of features that will define them among the global population of pegmatites.

The Cerný and Ercit classification (2005) is based on two concepts. Thus, the aplite-pegmatite veins in this area belong to rare elements class, according to the first concept, and to the LCT family according to the second concept.

When we divide the pegmatites into five classes (abyssal, muscovite, muscovite - rare elements, rare elements and miarolitic) we are defining an interval of pressure conditions, and also partly of temperature, that characterize the rocks in which they are hosted without necessarily reflecting the conditions of consolidation of the pegmatites themselves. These P-T conditions should be regarded as maximum estimates, since they correspond to the metamorphism peak that in many cases precedes the

pegmatites emplacement. As such, classifying these pegmatites as belonging to the rare elements class, it's assuming that they likely have settled at an intermediate to shallow depth and that when they become more fractionated they will tend to concentrate lithophile rare elements of economical interest (fig. 8).

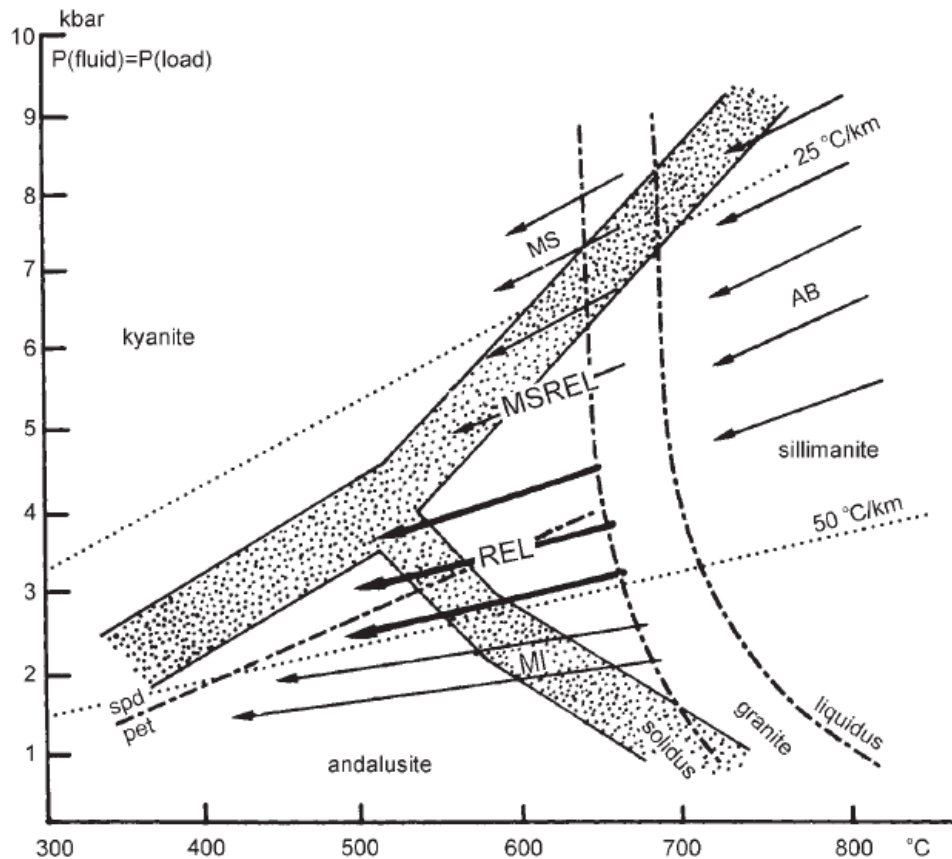


Fig. 8 - Schematic representation of the P-T fields of the pegmatites host rock, where you can observe the following classes: abyssal (AB), muscovite (MS), rare muscovite elements (MSREL), rare elements (REL) and miarolitic (MI). Arrows indicate regional fractionation trends present in pegmatites in relation to metamorphic gradients of the wall rocks. In some cases there are passages of a class to another, such as in cases of MS classes and MSREL, and in the cases of classes REL and MI (figure obtained from Cerny and Ercit 2005).

In particular, the members of the REL-Li subclass, where they were inserted, commonly are emplaced at low pressures (between the green schist facies and the amphibolite).

As previously mentioned, the aplite-pegmatite veins studied in this area were classified as complex type, spodumene sub-type and petalite sub-type. The complex type is precisely characterized by having a large amount of lithium aluminosilicates and may contain some of the most advanced structures and obtain some of the most extreme fractionation levels found in the earth's crust.

The spodumene subtype is the most common category of the pegmatite complex type. It's considered that these pegmatites usually crystallize at relatively high pressures ($\approx 3 - 4$ kbar).

The petalite subtype compared to the previous subclass is a smaller category, where the pegmatites of this type tend to crystallize sometimes at a bit higher temperatures and at lower pressures ($\approx 1.5 - 3$ kbar) than those of the pegmatite class of spodumene. However, these Li aluminosilicate may locally reflect the stage at which they reached saturation, instead of reflecting the pressure at which they were formed.

In general, the geochemical and paragenetics characteristics of these two subtypes are identical and usually have lower Li-content than those that were experimentally established as maximum.

According to the second concept of this classification, dividing the pegmatites in families is doing petrological and geochemical considerations of their origin. As such, this concept is different from the previous hierarchy, which had a more descriptive purpose, related to the geological environment.

Within the class of rare elements can therefore exist three families: NYF, LCT and NYF + LCT. NYF and LCT abbreviations correspond, respectively, to a family with a fractionation sequence enriched in niobium (Nb), yttrium (Y) + rare earth elements (REE) and fluorine (F) and a family with sequence fractionation enriched in lithium (Li), cesium (Cs) and tantalum (Ta).

The enrichment on these elements, within each pegmatite or population, of a given family, doesn't have to be proportional, nor occur evenly, and the assignment to a family of a pegmatite population doesn't mean that the elements of another family can't be present. However, these atypical phases occur in insignificant quantities when compared with the signature minerals of a particular family.

The LCT family usually contains, and progressively gets richer, in Li, Rb, Cs, Be, Ta, Nb ($Ta > Nb$) and in large part in B, P and F, as fractionation occurs in the melt.

In conclusion, Cerný and Ercit (2005), states that the two main sources of LCT parental melt are the anatexis of the metasedimentary and metavolcanic protoliths of the upper- to middle-undepleted crust, and a low percentage anatexis of (meta-) igneous rocks from the basement, or a mix of both (Cerný and Ercit, 2005).

Chapter 3 – Desk work with ArcGIS software

One of the goals of this study was to define catchment basins to which Li-contents, obtained through the analyses of stream sediments collected in previous studies of the Aplite-Pegmatite Field of Barroso-Alvão, could be assigned. Using this methodology it was possible to create a probability map of the Li-rich areas.

The chosen software was ArcGis v. 10.3. It was necessary to have a points shapefile, in which each point marks the location where each catchment basin area starts being defined, and a flow direction raster-based file from the region in study. With these two files it's possible to create a raster-based file of the catchment basins in the area of interest, using the *Watershed* tool from ArcGis software.

The points shapefile chosen to do this procedure was a shapefile with the location of 654 stream sediments sampling points, obtained through a previous study (Pires, 1995), containing in its table of contents, the content values of Li, Sn W, Nb, Ta and U, obtained in the analysis of each sample. The name of this shapefile is "SS" (stream sediments).

The flow direction raster image used was "d108_mod_esc", provided by the National System of Environmental Information (Sistema Nacional de Informação de Ambiente – SNIAmb). It had a pixel size of 25 m x 25 m (retrieved from SNIAmb, 24 Feb. 2016:

http://sniamb.apambiente.pt/infos/shpziips/D108_MOD_ESC_25_PTCONT_20790.zip).

The coordinate system used in this project was Hayford-Gauss, datum Lisboa.

In order to reduce the percentage error when constructing the catchment basins, waterlines were created through the flow direction image "d108_mod_esc", to adjust the "SS" points to the higher water accumulation areas from this image. The spatial analyst tools *Flow Accumulation* and *Set Null* were used to create the waterlines. To restrict the waterlines to the study area, the flow direction image (FD) was cropped with the *Clip* tool (from *Data Management Tools* section), overlapping the "SS" shapefile area. In the resultant new image, "clip_flow", the values with no data were defined as "0" (fig. 9B).

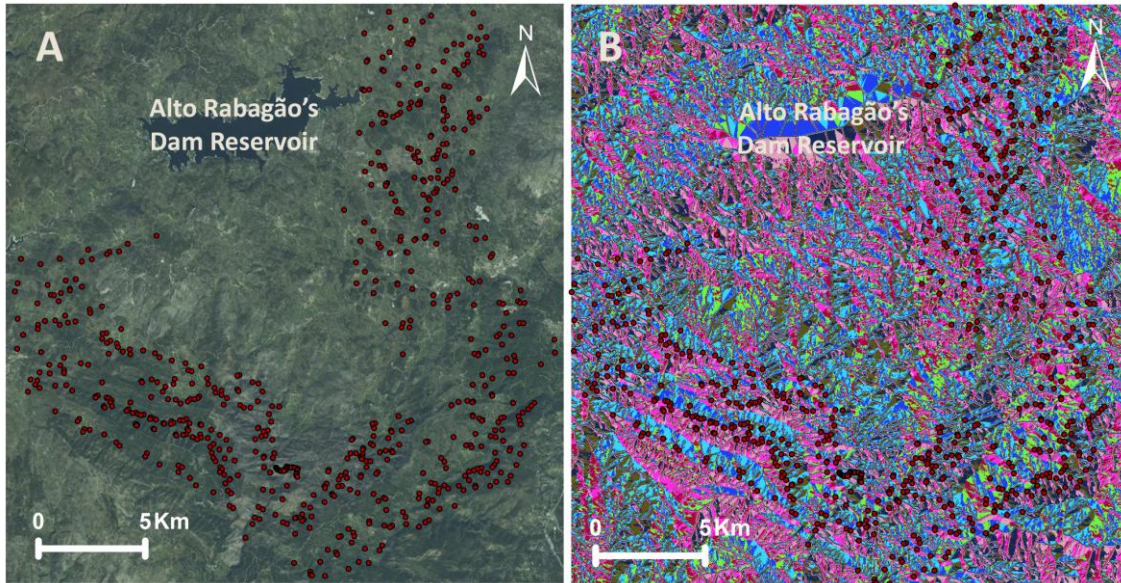


Fig. 9 - (A) Satellite image of the study area retrieved from the "World Imagery" map service of ArcGIS v. 10.3. (B) Representation of the flow direction image within the study area ("clip_flow"). The dark points represent the "SS" points.

Therefore, the *Flow Accumulation* tool (from the *Spatial Analyst* section) used the flow direction image (fig.9B) to create another raster image, in which higher values were assigned to the places (pixels) that had higher water accumulation, while lower values were assigned to the places with less water accumulation.

The pixels values of the resulting file were divided in two classes: 0-70 (black colored pixels) and 70-479464 (white colored pixels), where 479464 was the highest value attributed by this tool. The 0-70 class was created because all the values that were below 70 were of minor importance, since they correspond to zones of very little water accumulation. This way it was possible to have a better clue of the final appearance of the waterlines. The resulting raster image was named "flow_accum" (fig. 10).

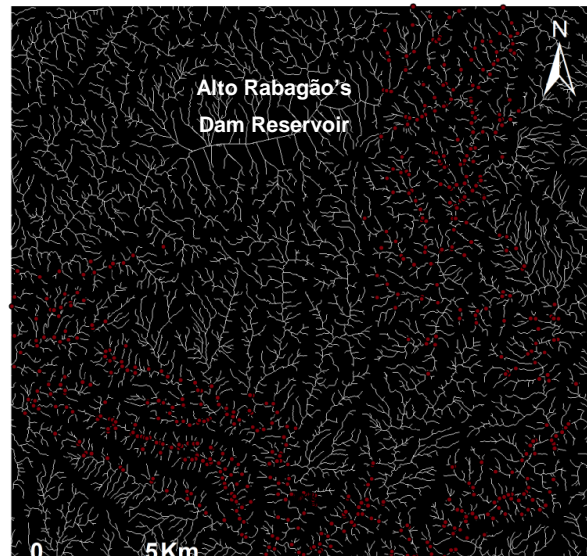


Fig. 10 - Representation of the "flow_accum" raster-based file that resulted from the "Flow Accumulation" tool. The black pixels represent the 0-70 class and white pixels represent the 70-479464 class, allowing the view of the waterlines. The red points represent the "SS" points.

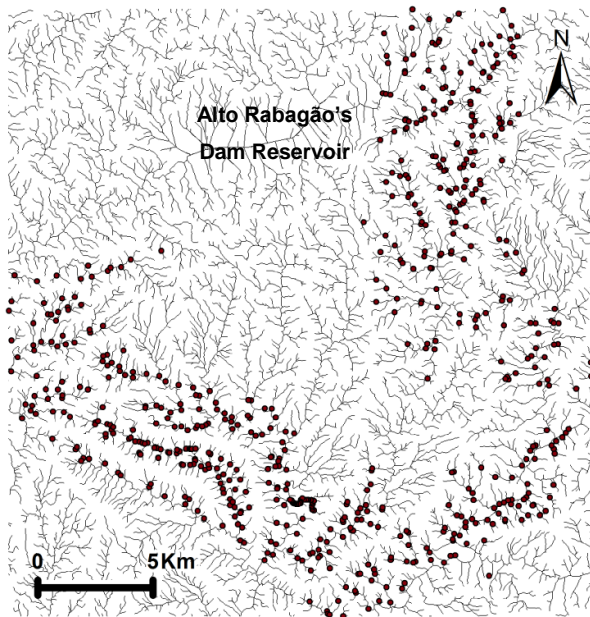


Fig. 11 – Representation of “SetNull” raster-based file that resulted from the “Set Null” tool. The black pixels have a value of 1 and represent the waterlines within the study area. The dark points represent the “SS” points.

The next step was to use the *Set Null* tool (from the *Spatial Analyst* section) to set, from the raster image “flow_accum”, that the pixels values under 70 were to be considered null (“value” < 70) and that the remaining pixel values would have a value of 1. The resulting raster image was named “SetNull” and represents the waterlines.

In order to use the *Watershed* tool it was necessary to manually adjusted the stream sediments sampling points to overlap the newly formed waterlines, to avoid errors to

happen, since the “SS” points need to be right in the zones of highest water accumulation, of the FD file, to correctly create the catchment basins.

To verify that the “SS” shapefile was really overlapping the raster waterlines, the “SS” points were also converted to a raster-based file.

Finally, it was possible to use the *Watershed* tool (from the *Spatial Analyst* section), with the adjusted “SS” points and the “clip_flow” image, to obtain a raster image of the catchment basins. The resultant file was named “bacias_raster” and was then converted into a vector-based file (polygons) in order to transfer the attributes with the Li-contents from the “SS” points, to the new catchment basins shapefile.

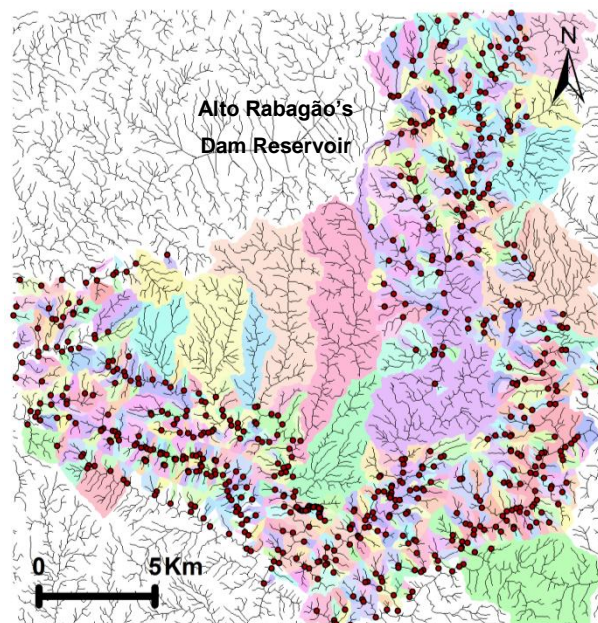


Fig. 12 – Representation of the catchment basins raster image (“bacias_raster”) resultant from the *Watershed* tool. Each color represents one catchment basin that was created from a “SS” point and from the “clip_flow” raster image, that provided the information about the flow direction according to the terrain topography. The dark points represent the “SS” points and the gray lines represent the waterlines.

However, during the conversion of the raster-based file, of the catchment basins, to a shapefile, some of the catchment basins polygons have been divided into small individual ones that should not exist, corresponding to individual pixels from the previous file, that had 625m² of area (fig. 13). Therefore, it was necessary to merge them in order to form the entire basins again. For this, the *Dissolve* tool (from the *Data Management Tools* section) was chosen and the catchment basins that had the same value in the “grid code” column, of the shapefile attribute table, were merged since each catchment basin had one value obtained from the previous file, “bacias_raster”. The new catchment basins shapefile was named “bacias_hidro_dissolve”.

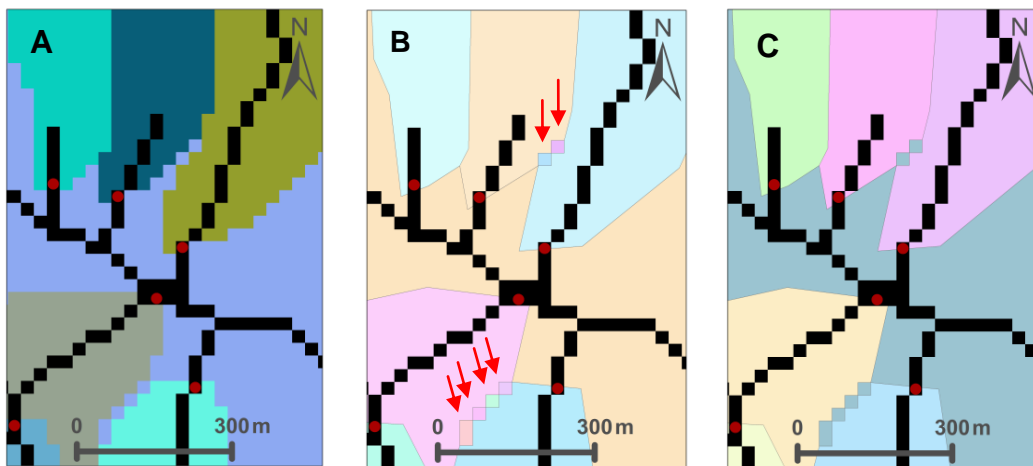


Fig. 13- Conversion errors from the raster image to the shapefile. (A) Representation of the catchment basins raster-based file. (B) Representation of the result of the conversion to a shapefile with the resulting subdivision of some catchment basin polygons into small individual ones. (C) Representation of the new and corrected catchment basins shapefile. The red points represent the “SS” points and the black lines represent the waterlines.

The next step was to use the *Spatial Join* tool (from the *Analysis Tools* sector) to copy the data with the Li-contents from the “SS” points to the new catchment basins. To do this, the “Contains” option was used so that when the "SS" points were inside the "hydro_dissolve" polygons, the attributes of the points were transcribed to the polygons of the basins. The resulting vector file was named "bacias_dren_final".

In the properties, within the symbology field, the Li-contents of the catchment basins were separated into seven classes, each one with a different color. According to Pires (1995) the background was considered as being 50%, the anomaly threshold as 84% and the anomaly as 97.5%. This way, the percentiles used were 50%, 75%, 84%, 90%, 95% and 97,5% which are respectively 99ppm, 134ppm, 156ppm, 186ppm, 229ppm and 267ppm. However, all the values starting from 50% must be taken into account as potential locations for Li-mineralized veins.

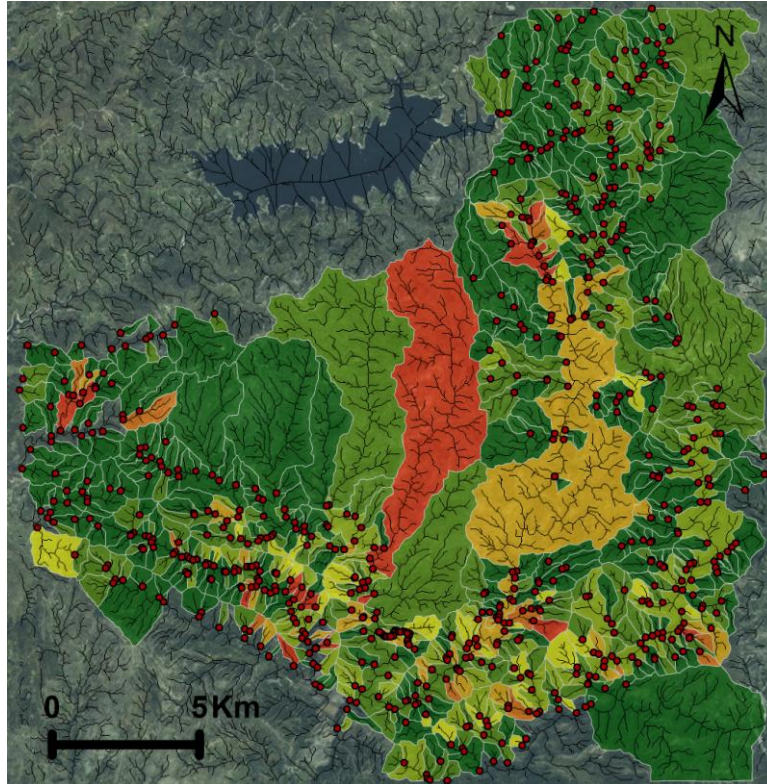


Fig. 14 – Representation of “Bacia_dreno_final” file, where each color represents a different class of Li contents.
The red points are the “SS” points and the black lines are the waterlines.

The Li-contents were separated in the following classes:

- 38.000000 - 99.000000
- 99.000001 - 134.000000
- 134.000001 - 156.000000
- 156.000001 - 187.000000
- 187.000001 - 230.000000
- 230.000001 - 267.000000
- 267.000001 - 635.000000

The catchment basins that had an area over 2 km² were eliminated or cut because they were created due to lack of information, as there were no more stream sediments sampling points in those locations (final image result in Annexes 1).

It should be taken into account the Li-barren granites and the areas that are overlapping them, since they are not to be considered as likely zones to contain Li-mineralized veins.

Chapter 4 – Field work and sampling

The studied veins are aplite-pegmatites because they have both aplite texture and pegmatitic texture. It's often assumed that crystal size directly indicates the degree of growth rate and magma cooling rate, being the small crystals derived from a quickly cooling magma and the large crystals derived from a magma that has cooled slowly, however, according to Webber (2007), this doesn't explain what really happens in many pegmatite bodies, especially in the aplite-pegmatite bodies where a strong cooling variability would be required.

Therefore, it seems that the crystallization parameters, such as nucleation and growth rates, couldn't always be the same during the formation of these aplite-pegmatite veins. Events such as melt emplacement into a relatively cold country rock (quench thermal), a chemical quench caused, for example, by the crystallization of tourmaline, which can effectively remove boron from the melt, or rupture or dilatation of a body (pressure quench), may increase the degree of melt undercooling and can start an destabilization of the crystallization dynamics in a pegmatite system. Thus, these events can initiate rapid heterogeneous nucleation and an oscillatory crystallization, such as development of a layer of excluded components on a crystallization front (Martins, 2009; Webber, 2007; Webber *et al.*, 2005).

In Barroso-Alvão aplite-pegmatite field the aplite-pegmatite veins only appear in sintectonic two-mica granites and in early Paleozoic metasediments, but only some of the veins emplaced in the metasediments of Rancho sub-unit and Santa Maria de Émeres unit, belonging to the Carrazedo Structural Domain, have Li-mineralizations.

This aplite-pegmatite population has no apparent spatial zonation, both barren and Li-mineralized aplite-pegmatite veins appear within the same metasedimentary rocks, from the same lithostratigraphic units. They show up as countless aplite-pegmatite veins and locally appear in dense swarms of more than 10 bodies, with different lengths and thicknesses, that sharply cross-cut the metasediments (Charoy and Lhote, 1992; Martins, 2009; Lima, 2000).

During the field work done in this area 12 Li-mineralized aplite-pegmatite veins were observed, as well as 4 old mines from where Sn used to be obtained. Of the first 12 veins, 10 are from the Rancho sub-unit and 2 from the Santa Maria de Émeres unit (fig.15). All the coordinates of this aplite-pegmatite veins can be found in Annex 2.

Some veins are controlled by the S_2 foliation and may be locally deformed by D_3 ($N120^\circ$), but some others are also be controlled by D_3 -related planes. This seems to indicate that the emplacement of the pegmatitic melt was structurally controlled during

the peak of metamorphism, from ante-D₃ to sin-D₃ (Noronha, F. *et al.*, 2013; Charoy *et al.*, 1992; Martins, 2009).

However, there are some veins that also appear to have filled sub-horizontal and sub-vertical fracture systems like shear fractures, as veins can be found parallel to each other, possibly echelon structures. This suggests that the melt installation would also have occurred after the peak of metamorphism, during a later and less ductile phase. Lima and Noronha (2006) also states that the installation of the melt could have occurred during and after the peak of metamorphism.

Recent studies from Dakota Minerals (2016b) also state that some pegmatites appear to be curved in folds with vertical axis to slightly recumbent, with thicker pegmatites commonly developed in the fold nose of NW anticlines.

The Li-mineralized aplite-pegmatite veins have a mineralogical composition identical to a granitic composition. According to Martins (2009), the veins are mainly composed of feldspars, up to 50 cm in length, uniformly distributed or forming swarms, spodumene and/or petalite single or in clustered crystals, and small rounded grains of quartz.

The spodumene has a pearl-white color and can have up to 30 cm in length. The petalite is almost transparent when it is fresh and has a light yellowish color when weathered.

As accessory minerals, the most common is moscovite, with centimeter size, but there are also montebrasite, apatite, tourmaline, cassiterite, columbo-tantalite, clay minerals and Fe and Mn oxides.

The cassiterite can be primary (cassiterite I) or secondary, of hydrothermal origin (cassiterite II). Primary cassiterite was found as an accessory mineral of petalite dominant veins and had deformation. As such, possibly, in the maps with Li- and Sn-contents (obtained according to the methodology described in chapter 3), the zones that are anomalous in both elements, would have a higher probability of containing petalite veins. However, it is possible that due to the great Sn demand that existed in this region, currently the stream sediments in certain areas have been washed by the population to obtain this ore (Lima, 2000, Lima *et al.*, 2003, Martins *et al.*, 2007).

In field work, several andalusite porphyroblasts were also observed in the metasediments, as described by Lima (2000) by M.A. Ribeiro (1998), who described the DEC units as having a degree of metamorphism corresponding to the biotite zone,

where these large crystals can be found. It was also observed that is common to find exudation quartz in the metasediments.

The data collected in this study is now part of the Barroso-Alvão database (pegmatitos_barroso.dbf), that also contains data from geological charts 1: 50000 (6A, 6B, 6C and 6D) and from several other researchers that already have studied the area.

Some of the aplite-pegmatite veins presented in this work were already known for their contents in Li, but others, weren't yet identified as being Li-rich or weren't yet identified at all. These were found using the results of the desk work referred in Chapter 3.

In the following figures are represented the locations of the 12 Li-mineralized veins observed in the field, together with the representation of the Li-bearing (fig.15) and Sn-bearing (fig. 16) catchment basins, as well as the mining concessions that can be found here. The maps were created in ArcGIS v. 10.3, using 6C - Cabeceiras de Basto 1: 50000 sheet and 6D - Vila Pouca de Aguiar 1: 50000 sheet of the Geological Map of Portugal. The colors chosen to represent Sn-contents range from dark green to red, with the darkest green corresponding to the "regional background" (percentile of 50%), the lighter green to the "anomaly threshold" (percentile of 84%) and the reddish orange to the "anomaly" (percentile of 97.5%).

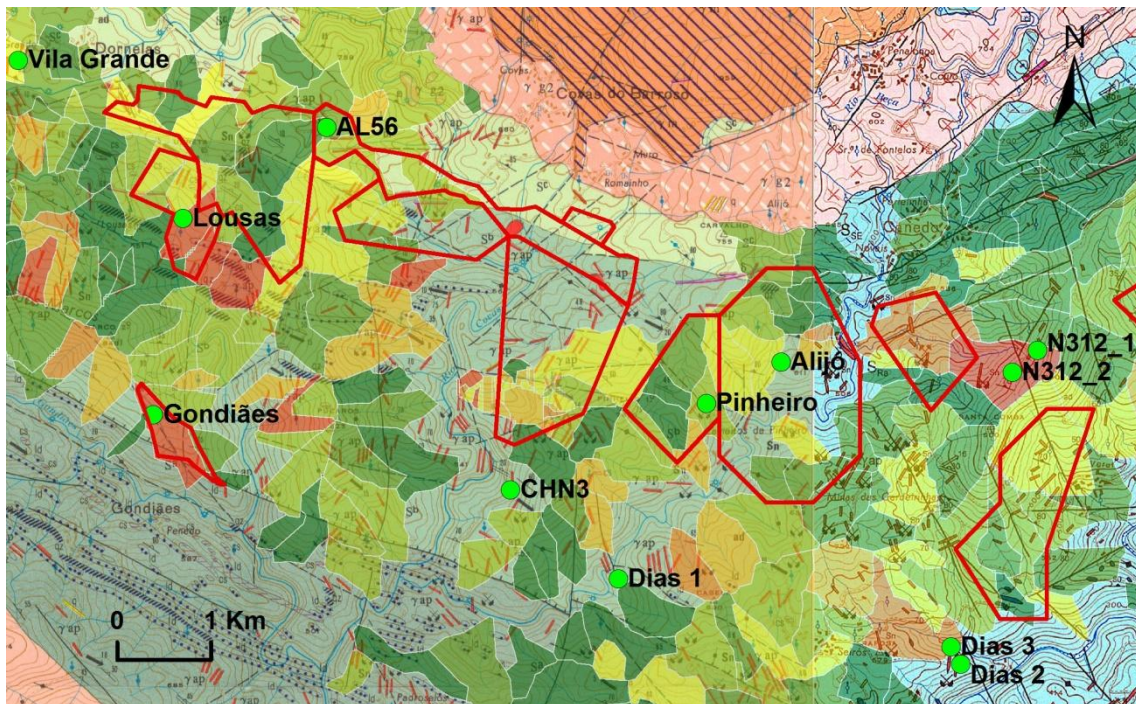


Fig. 15 - Locations of the 12 Li-mineralized veins observed in the field, together with the representation of the Li-bearing catchment basins, as well as the mining concessions that can be found here. The maps were created in ArcGIS v. 10.3, using 6C - Cabeceiras de Basto 1: 50000 sheet and 6D - Vila Pouca de Aguiar 1: 50000 sheet of the Geological Map of Portugal.

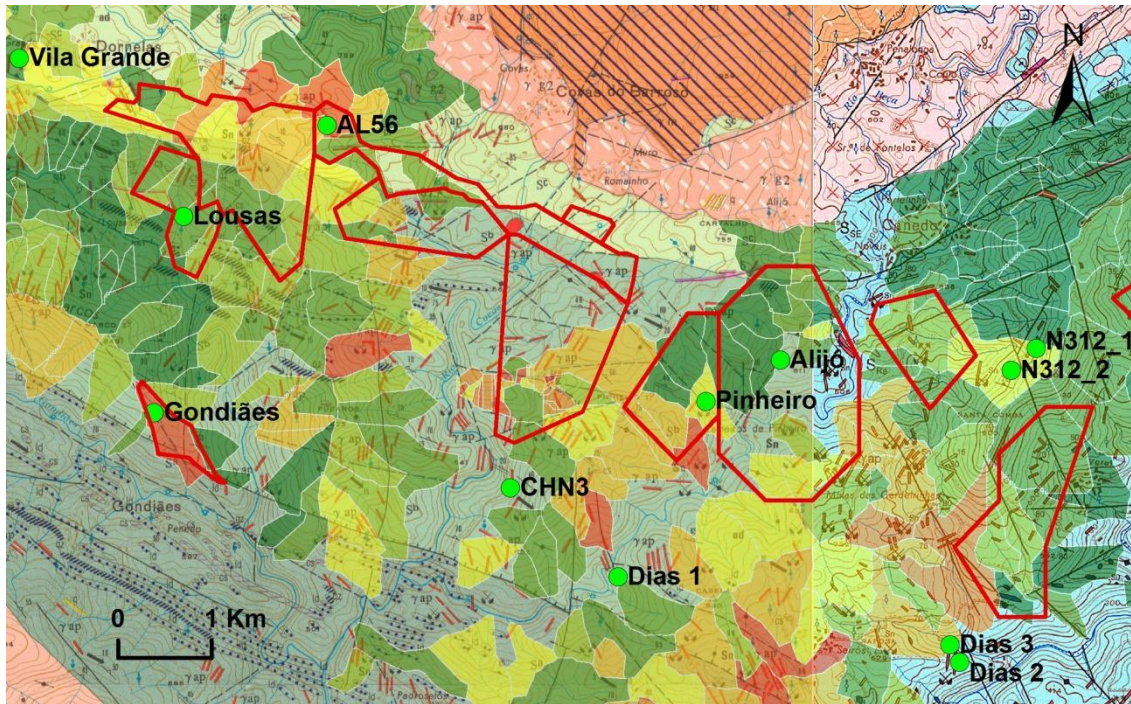


Fig. 16 - Locations of the 12 Li-mineralized veins observed in the field, together with the representation of the Sn-bearing catchment basins, as well as the mining concessions that can be found here. The maps were created in ArcGIS v. 10.3, using 6C - Cabeceiras de Basto 1: 50000 sheet and 6D - Vila Pouca de Aguiar 1: 50000 sheet of the Geological Map of Portugal.

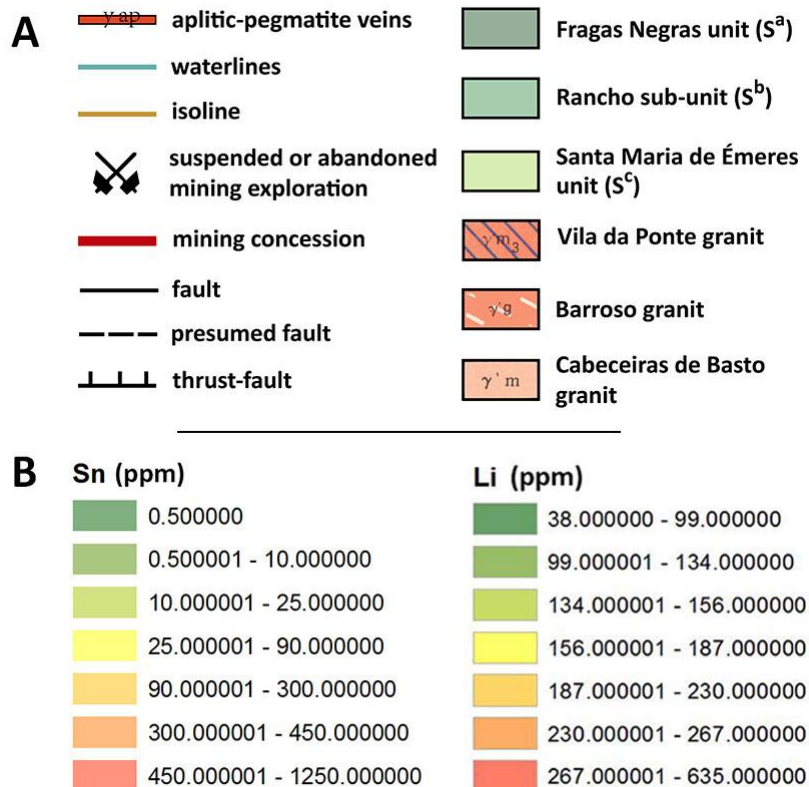


Fig. 17 – (A) Legend with the symbols, structures and lithostratigraphic units from the geological maps shown in fig. 15 and Fig. 16, corresponding to sheet 6C - Cabeceiras de Basto, scale 1: 50000. (B) Li- and Sn-content classes used in the representation of the catchment basins from fig. 15 and fig. 16.

4.1. N312-1 and N312-2 aplite-pegmatite veins

Both the N312-1 and the N312-2 aplite-pegmatite veins were first indicated as having a high probability of being Li-mineralized by the Li-bearing catchment basins from Chapter 3. These are emplaced in Rancho sub-unit metasediments that have a foliation of N120°; subvertical (to north), that is typical found as D₃ regional orientation.

The N312-1 aplite-pegmatite vein is quite weathered and has an 8.4m width. Despite the weathered appearance, as it seemed to be able to contain relics of old Li-minerals and was within an area with high content in Li (fig. 19), some samples were collected in order to prepare thin sections (P1a, P1b, P1c and P1d) that were later observed under the petrographic microscope.

The resultant thin section was very weathered, as was already expected, but they gave the confirmation that this vein was actually mineralized, since relics of petalite, amblygonite and cookeite were found.

In the field, this aplite-pegmatite vein appeared to have an orientation of about N70°.

The N312-2 aplite-pegmatite vein is subhorizontal, and is also very weathered. It seems to have some Li-content indicated by the pink colored alteration of some minerals.

In this vein there are feldspar crystals growing in a comb structure from the aplite-pegmatite contact with the country rock (fig.18).



Fig. 18 – Feldspar crystals growing in a comb structure from the aplite-pegmatite (N312-2) contact with the country rock.

According to Webber (2007), London (1992) states that when a progressively larger liquidus undercooling of a hydrous silicate melt occurs, the crystals cease to have a random orientation and begin to orient themselves in a comb structure.

Webber (2007) also states that an important characteristic in pegmatites is the textural heterogeneity they display with respect to crystal morphologies, being that the

textural relations within the pegmatites minerals reflect the pegmatite undercooling degree, nucleation rate and growth rate. A strong undercooling is required to explain many textural characteristics of pegmatites, such as the development of comb structures along the pegmatite contacts with the country rock. This is what seems to happen in this aplite-pegmatite vein.

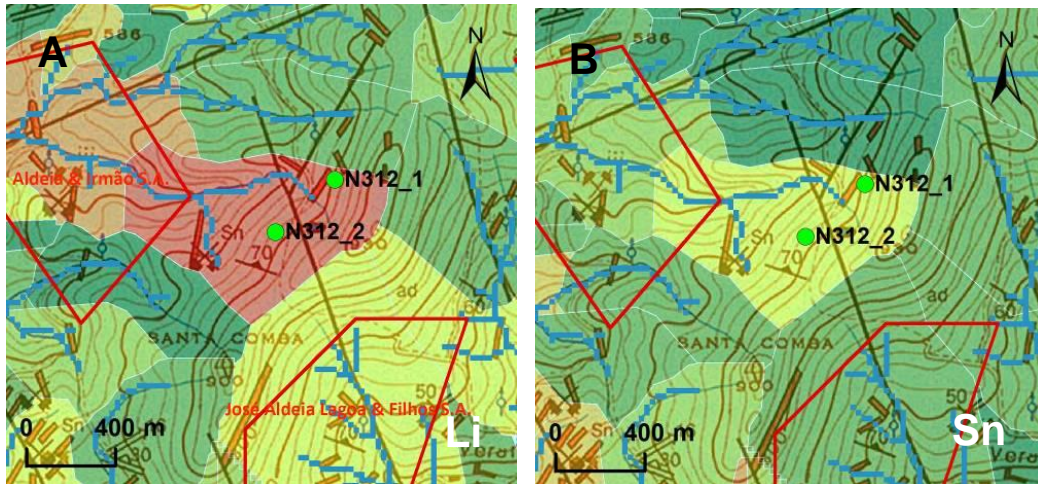


Fig. 19 – Localization of N312-1 and N312-2 aplite-pegmatite veins on the Li-bearing (fig. 19A) and Sn-bearing (fig. 19B) catchment basins maps, using 6D - Vila Pouca de Aguiar sheet of the Geological Map of Portugal. The blue lines represent the waterlines.

According to the analysis of the Li-bearing and Sn-bearing maps, these aplite-pegmatite veins are inserted in a catchment basin with high Li-contents and that also has some important Sn-contents. With only this analysis it was already possible to assume that this vein could be a petalite one, but the petrographic analysis from N312-1 vein also possessed petalite relics. Therefore, the results of this analysis are within expectations.

4.2. CHN3 aplite-pegmatite vein

The CHN3 aplite-pegmatite vein is subvertical and in general it possess an azimuth of N150°. However, a contact between the schist and the aplite-pegmatite was measured with an attitude of N120 °; SV.

This is a Li-mineralized body, and contains spodumene crystals, that can be seen in the outcrop visited more southerly, but it also contains petalite crystals further north still in the same outcrop.

A petalite sample was collected (fig. 20) and later analyzed by the Scanning Electron Microscope (SEM) at the Materials Center of the University of Porto (CEMUP), where its identification was confirmed by the Al/Si relation, which is only compatible with this mineral.



Fig. 20 – Petalite crystal from CHN3 aplite-pegmatite vein.

According to Charoy *et al.* (1992), this vein is cross-cut by several late-D₃ shear-zones, 3-5 cm wide, and was known as being only mineralized in spodumene. During this 1992 study, thin sections were made with the purpose of containing some shear-zones. These thin sections were reanalysed in the course of this dissertation.

During the field work it was possible to see shear-zones cross-cutting the aplite-pegmatite vein and to notice that these are right-lateral. In this case, there were shear-zones with attitude of N132 °; SV that were cut by later shear-zones with attitude of N162 °; SV (fig. 21). Moreover, there was a small shear-zone, about 1cm wide, filled with quartz and with spodumene on the edges (fig. 22). This spodumene is posterior to the one previously observed, like what was seen in the mentioned thin blades from Charoy *et al.* (1992).

The local metasediments also have a very fine and well marked foliation, again indicating the presence of a 3rd phase shear corridor (D₃). In addition, there were andalusite porphyroblasts also deformed by these shear-zones in the vicinity.

This aplite-pegmatite vein isn't covered by the Li-bearing map produced in Chapter 3 because no sample of stream sediments was collected in the secondary waterline that would outline the catchment basin of this area.

However, this body contains cassiterite (seen in thin section) and, therefore, this area should contain high contents of Sn and Li.

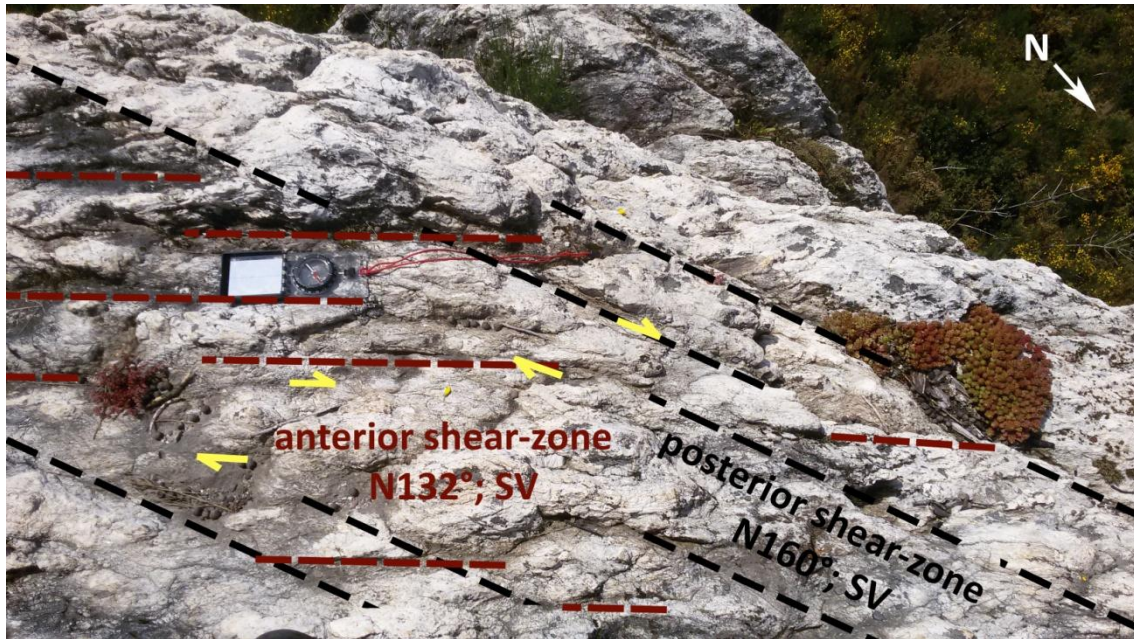


Fig. 21 - Two shear-zones cross-cutting the aplite-pegmatite vein: a shear-zone with attitude N132 °; SV and a later one with attitude N160 °; SV. Both are right-lateral (indicated by the yellow arrows).

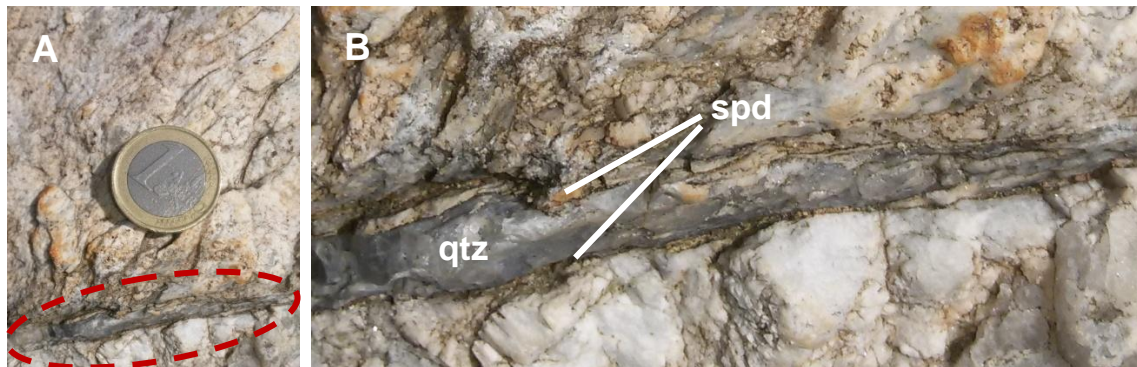


Fig. 22 - (A) Small shear-zone filled by quartz and with spodumene in the edges, observed in CHN3 aplite-pegmatite vein. (B) Close-up of the shear-zone represented in fig. 22A.

4.3. Alijó aplite-pegmatite vein

Alijó aplite-pegmatite vein belongs to José Aldeia Lagoa & Filhos, SA. mining concession.

In the exploration zone of "Alijó vein" there are two sub-parallel, aplite-pegmatite veins with an azimuth of N165° and a variable inclination of 45°W to 60°E. The exploration is being carried out on the largest vein, on the west side (between 5 m and 45 m of width).

According to Farinha (1998) this vein must have at least 380 m of extension.

Despite the fact that at the exploration site the vein seems to be a continuous body, according to the survey results from previous studies, the vein has a schist enclave, in depth, which displays the same deformation as the schist of the country rock (Lima, 2000).

According to Professor Fernando Noronha (personal communication, 2016) these veins emplacement seems to have been controlled by a shear zone.

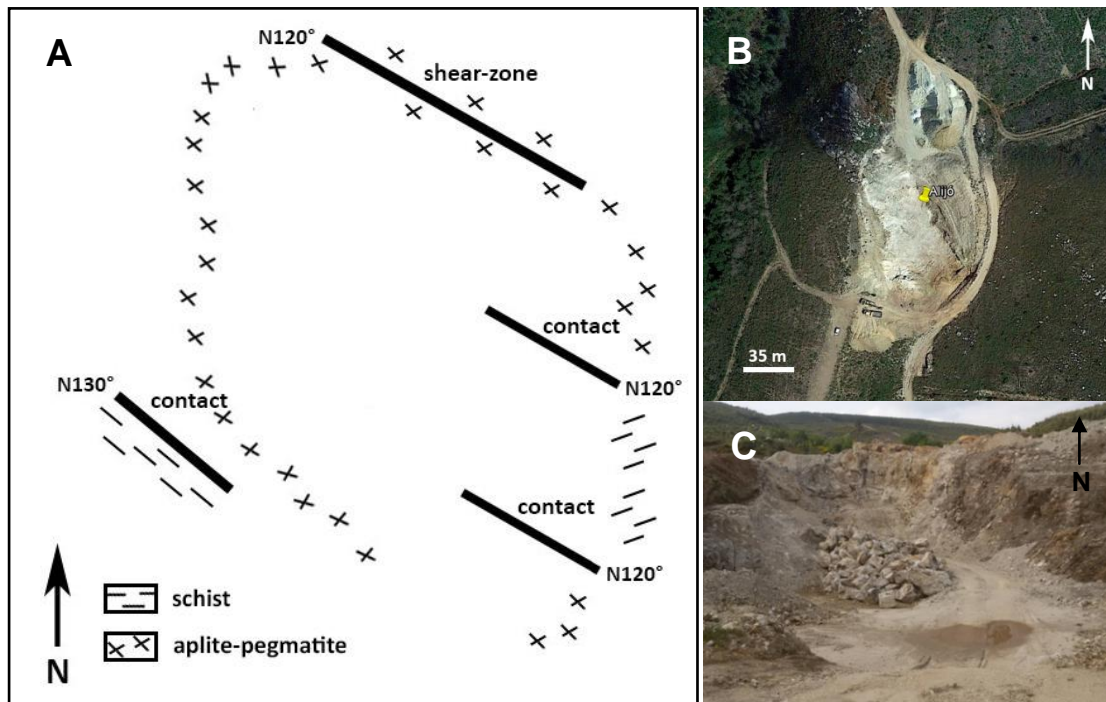


Fig. 23 – Alijó aplite-pegmatite vein exploration site. (A) Exploration site photo. (B) Satellite image of the exploration site. Google Earth adapted image. (C) Schematic figure representative of the contacts directions observed in the exploration site of the aplite-pegmatite vein and of a shear plane located north of the exploration.

In this location, the metasediments were very deformed, with azimuths from N70° to N160°, indicating the presence of a D₃ shear corridor (fig. 24). This goes along with the observations that were made in Lima (2000), where it was stated that the

metasediments are marked by D_3 , with directions from $N120^\circ$ to $N140^\circ$. According to this study, andalusite crystals of ante- D_3 , were also observed.



Fig. 24 – D_3 shear corridor at the exploration site of Alijó aplite-pegmatite vein

As previously reported, in the aplite-pegmatite vein exploration site, only spodumene crystals were seen (fig. 25) and no petalite was found. It's also stated that spodumene aplite-pegmatite veins, like this one, usually have higher Fe-contents than

those of petalite. Spodumene aplite-pegmatite veins usually have low Sn-contents, like what happens with this vein (Martins et al, 2007).

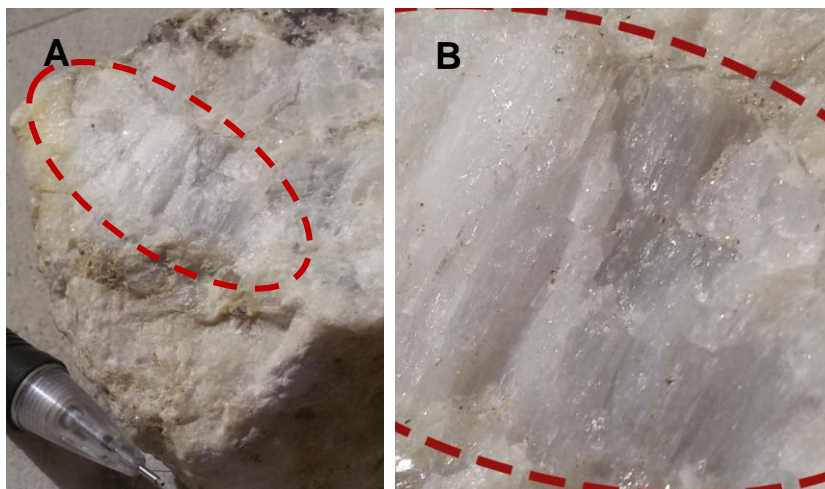


Fig. 25 – (A) Collected sample with several spodumene crystals. (B) Close-up of fig. 25.A.

In this aplite-pegmatite vein it's possible to see the aplitic texture and the pegmatite texture occurring alternately. Within the aplitic portion there were bands rich in small crystals of tourmaline.

Locally an interesting orientation of the crystals ($N70^\circ$) is observed, which could indicate a preferred orientation of the spodumene crystals, but in general the crystals show a random direction such as $N60^\circ$, $N40^\circ$ and $N90^\circ$.

In the enclosing schists, there are millimetric tourmaline crystals near the aplite-pegmatite vein. They could have been formed due to the mutual contribution of the aplite-pegmatite and the schist, being that the first would have provided the B and the second the Mg. Supporting this idea is the fact that it was not found tourmaline in quartzitic zones because the Mg would have come from the biotite in the schist.

Already in Martins (2009) was referred the occurrence of tourmalinization in the metasediments that were near the contacts with the pegmatites emplaced in Rancho sub-unit and Santa Maria de Émeres unit. In Lima (2000), it is also mentioned that Ramos (1998) stated that the intense tourmaline crystallization could have happened thanks to the released of B from the pegmatitic melt to the country rock.

Alijó aplite-pegmatite vein is also not covered by the Li-bearing and Sn-bearing catchment basins maps. The catchment basin where this vein was in, was a basin with several kilometers belonging to a main water stream (the Beça river), meaning that the stream sediments collected there were a mixture of sediments brought by other water courses.

4.4. Pinheiro aplite-pegmatite vein

The Pinheiro aplite-pegmatite vein belongs to the Aldeia & Irmão S.A. mining concession and it is also within the metasediments of Santa Maria de Émeres unit. This is a subhorizontal vein with spodumene crystals that can be 10 cm long (fig. 26B).

In this place the contact between the aplite-pegmatite vein and the country rock was visible with an N110°; SV attitude.

As for the contents of the catchment basin, where this vein is inserted, there is a high Sn-content, despite the fact that only spodumene was found during field work. However this may be explained because of the old Sn mines nearby.

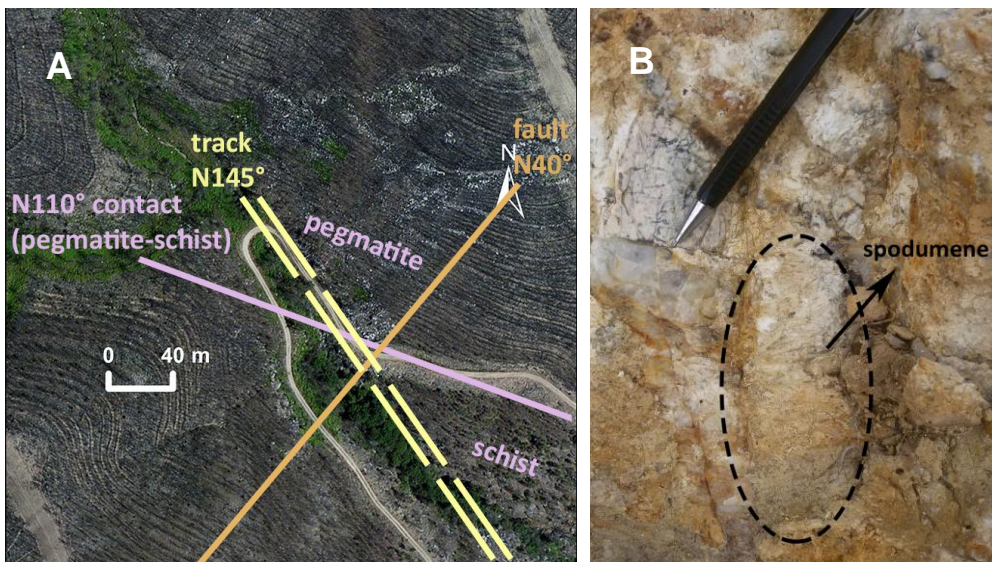


Fig. 26 - Pinheiro aplite-pegmatite vein. (A) Satellite image with the representation of the structural setting observed during field work. This image was adapted using the ArcGIS 10.3 World Imagery service. (B) Spodumene crystal.

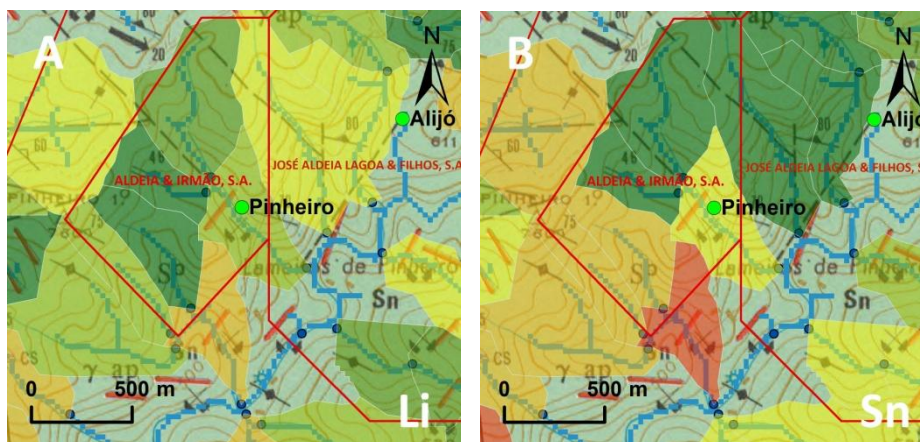


Fig. 27 - Location of Pinheiro aplite-pegmatite vein on the Li-bearing (fig.27A) and Sn-bearing (fig.27B) catchment basin maps, using the 6C - Cabeceiras de Basto sheet, from the Geological Map of Portugal. The blue lines and blue points represent the waterlines and "SS" points respectively.

4.5. Vila Grande aplite-pegmatite vein

Vila Grande aplite-pegmatite vein is very weathered, but it was still possible to find some petalite crystals, meaning that this one is Li-mineralized vein. Its attitude, measured in the field, is N110 °; 48 ° SW. It belongs to the metasediments of Santa Maria de Émeres unit.

In this vein a columbo-tantalite crystal was also found, later confirmed by a portable X-ray fluorescence device (XRF).

Previously, this aplite-pegmatite vein wasn't identified as Li-mineralized.

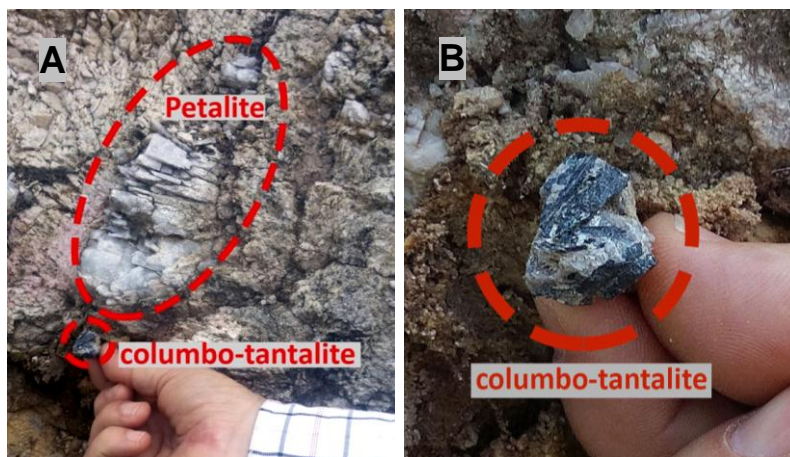


Fig. 28 - (A) Columbo-tantalite and petalite from Vila Grande aplite-pegmatite vein. (B) Close-up of the columbo-tantalite crystal from fig. 28A.

Although the Li-bearing and Sn-bearing maps show that this area has high Li-contents, the Sn- contents are only 0.5 ppm, despite their relation with petalite veins. It's possible that these values are due to the large Sn demand that occurred in this region, causing the stream sediments in certain locations to have been washed by the local populations.

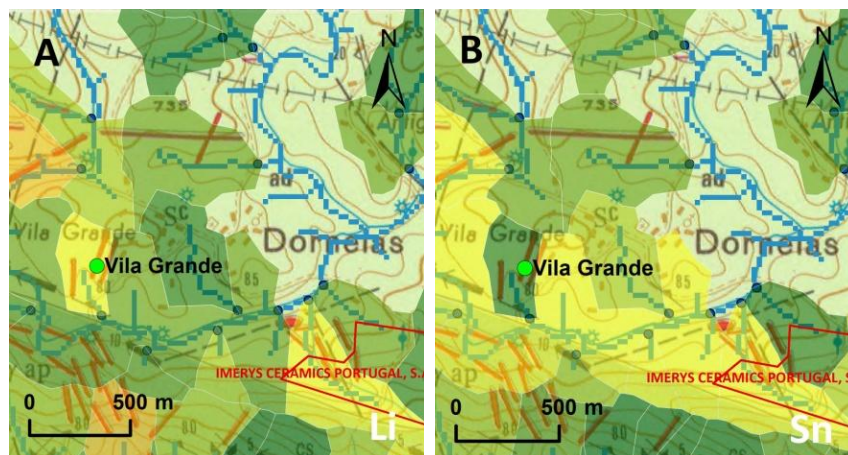


Fig. 29 - Vila Grande aplite-pegmatite vein location on the Li-bearing (fig. 29A) and Sn-bearing (fig. 29B) catchment basin maps, using 6C - Cabeceiras de Basto sheet, from the Geological Map of Portugal. The blue lines and blue points represent the waterlines and "SS" points respectively.

4.6. Lousas aplite-pegmatite vein

Lousas aplite-pegmatite vein belongs to Felmica Minerais Industriais, S.A. mining concession and is emplaced in Rancho sub-unit metasediments.

This vein is sub-horizontal ($70^{\circ}W$), and its azimuth varies between N-S and $N20^{\circ}$, making him discordant from the main fabric found in the surrounding metasediments, in other words from the F_3 crenulation cleavage.

In the exploration site, the Lousas vein shows 70m of maximum width (E-W) and 13 - 15m of depth. However, there are lateral branches with several meters in length that already have been recognized, which indicates that this aplite-pegmatite vein should have a total extension of about 500 m (N-S) (Farinha, 2012, Martins *et al.*, 2007).

The most abundant lithium mineral present in this aplite-pegmatite vein is petalite. Although, Professor Alexandre Lima (personal communication, 2016) states that there is spodumene at the southern and northern extremes of this vein.

Further north, still within the exploration site, there are some spodumene crystals with the characteristic fine cleavage, with quartz intergrowths that suggests SQI (Spodumene Quartz Intergrowth) (fig. 30). According to Lima *et al.* (2007), London (1984) states that petalite is stable at a temperature between $550^{\circ}C$ - $680^{\circ}C$ and at a pressure between 2 Kbar - 4 Kbar, being that below these temperatures the petalite decomposes into spodumene + quartz, forming what is known as SQI. Therefore, this spodumene would be posterior to the petalite.

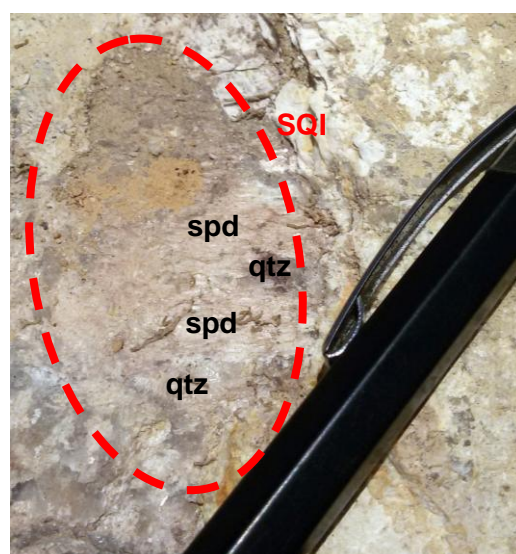


Fig. 30 - Spodumene with quartz intergrowths (SQI - Spodumene Quartz Intergrowth)

Close by, it was possible to find the direction of the pegmatite melt, shown by a crystallization front were the crystals have grown in the fluid movement direction. There were also broken petalite crystals nearby, which seemed to have been the first to crystallize in the melt, but then would have been pushed, resulting in scattered

fragments (fig. 33). Close to them there were also petalite crystals, but this time unbroken. These ones didn't have a preferential orientation such as most of the petalite crystals observed in this vein (fig. 31).

One of the fractures of this aplite-pegmatite vein has pink areas, corresponding to Li-rich altering minerals. This has already been seen previously in other Li-mineralized veins.

Concerning the probability map of Li- and Sn- contents, the catchment basin where this vein is inserted has a high Li-content, but very low Sn-contents (0.5 ppm), despite of this being a petalite vein and having old Sn mining works in this location (fig. 32). As such, it's possible that the stream sediments were washed to obtain Sn, as what may have happened in Vila Grande aplite-pegmatite vein.



Fig. 31 - Petalite crystals randomly distributed in Lousas aplite-pegmatite vein. In these crystals can be seen very well the translucent appearance of fresh petalite.

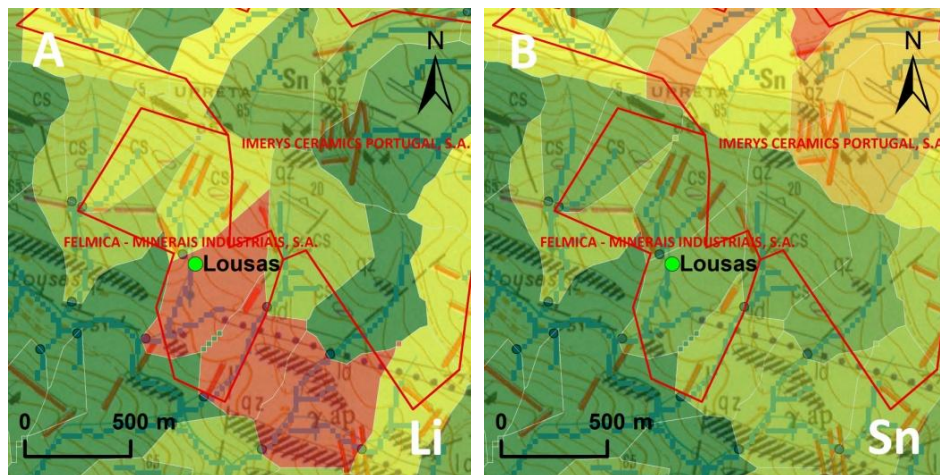


Fig. 32 – Location of Lousas aplite-pegmatite vein on the Li-bearing (fig. 28A) and Sn-bearing (fig.28B) catchment basin maps, using 6C - Cabeceiras de Basto sheet, from the Geological Map of Portugal. The blue lines and blue points represent the waterlines and “SS” points respectively.

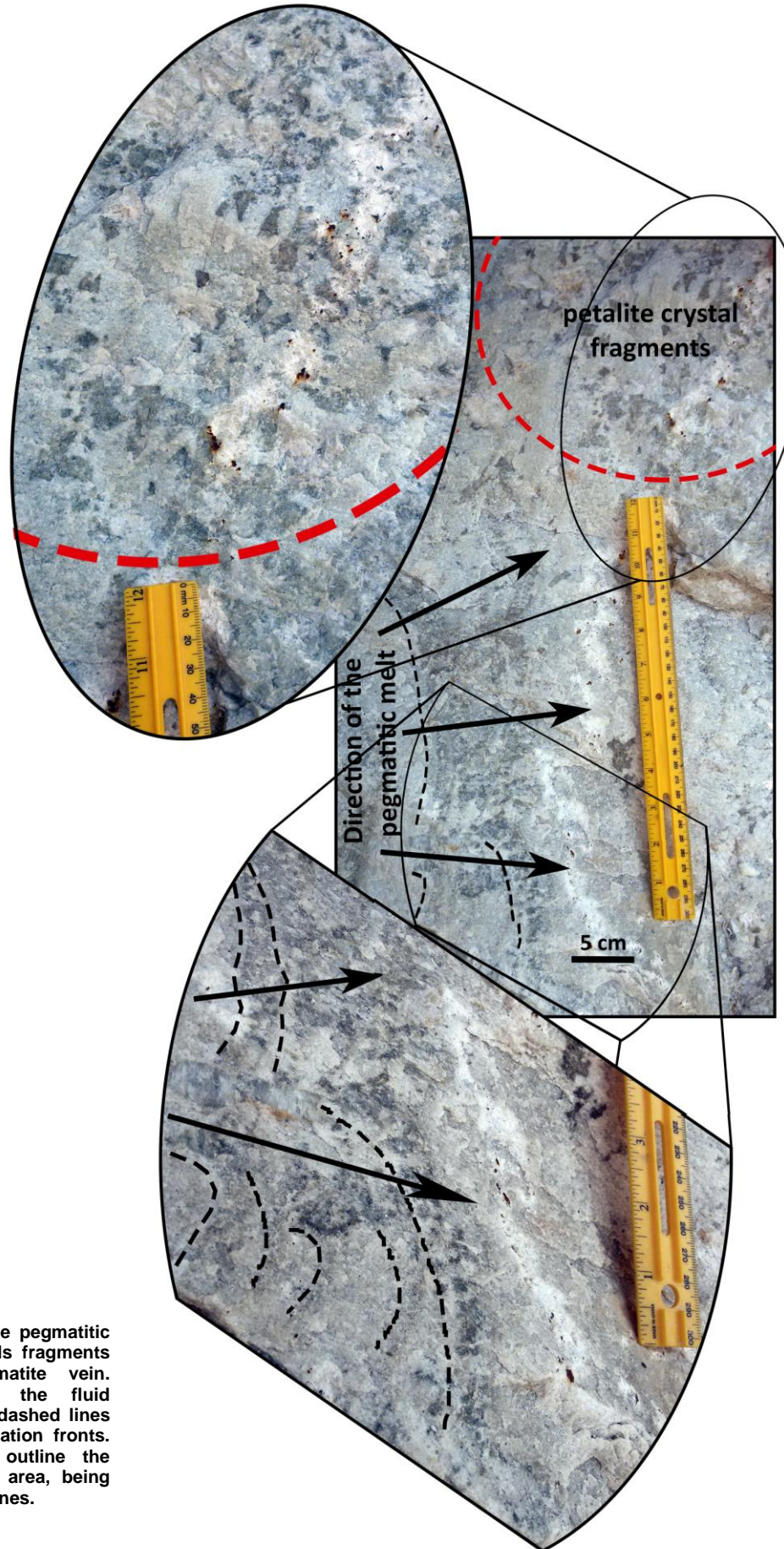


Fig. 33 - Direction of the pegmatitic melt and petalite crystals fragments of Lousas aplite-pegmatite vein. The arrows indicate the fluid direction and the black dashed lines represents the crystallization fronts. The red dashed line outline the petalite broken crystals area, being that they are the darker ones.

4.7. AL56 aplite-pegmatite vein

The aplite-pegmatite vein located in the AL56 vein area, emplaced in the metasediments of the Santa Maria de Émeres unit, belongs to Imerys Ceramics Portugal, S.A mining concession. This is sub-vertical and has an orientation of about N136°, like the main fabric of the surrounding metasediments.

In this vein there are many crystals of spodumene with quartz intergrowth (SQI) (fig. 35). Feldspars that, according to Professor Mona-Liza Sirbescu (personal communication, 2016), appear to have been deformed while the surrounding minerals would have melted and crystallized around them (fig. 29).

In this zone it was collected a sample of petalite passing to spodumene + quartz, from which thin sheets were made. Their petrographic analysis can be found in Chapter 2.



Fig. 34 - Deformed feldspars from the aplite-pegmatite vein located in the AL56 vein area.

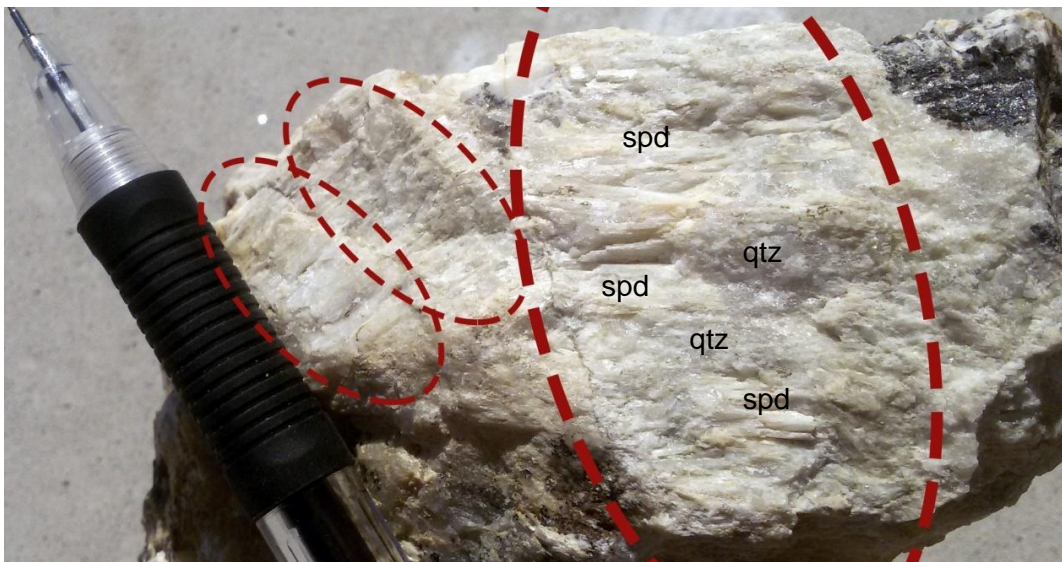


Fig. 35 – Sample with SQI crystals from the aplite-pegmatite vein located in the AL56 vein area.

According to the Li-bearing and Sn-bearing maps, this site, besides being indicated as an area that possibly contains Li-mineralized veins, is also indicated as having a large amount of Sn, which corroborates the fact that this vein was of petalite that was replaced by spodumene + quartz.

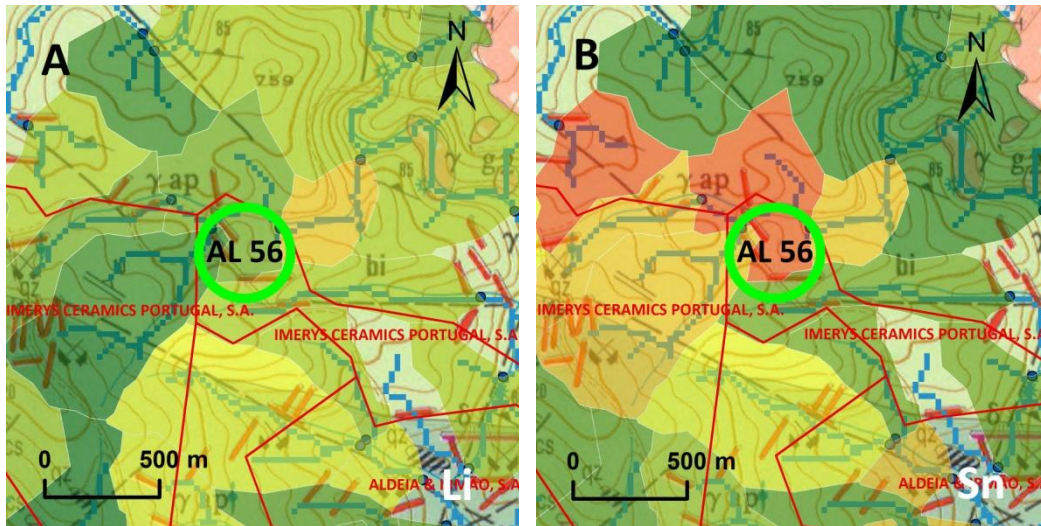


Fig. 36 - Location of the aplite-pegmatite vein present in the AL56 vein area in the Li-bearing (fig.36A) and Sn-bearing (fig.36B) catchment basin maps, using the 6C - Cabeceiras de Basto sheet, from the Geological Map of Portugal.

The blue lines and blue points represent the waterlines and "SS" points respectively.

4.8. Gondiaes aplite-pegmatite vein

Gondiaes aplite-pegmatite vein belongs to Felmica Minerais Industriais, S.A. mining concession, has about 950 m of extension and 45 m width. It's within the Rancho sub-unit metasediments.

The aplite-pegmatite vein is subvertical and has a direction around N30°. The main Li-mineral is petalite and it also has cassiterite that was already explored to obtain Sn (Internal Report Felmica, 2004).

According to Professor Alexandre Lima (personal communication, 2016), this aplite-pegmatite vein, like the one from Lousas, also has spodumene in its southern and northern extremes.

The analysis of the Li-bearing and Sn-bearing maps makes it easy to assume the presence of petalite veins, since they contain high Li-contents and high Sn-contents (fig. 37).

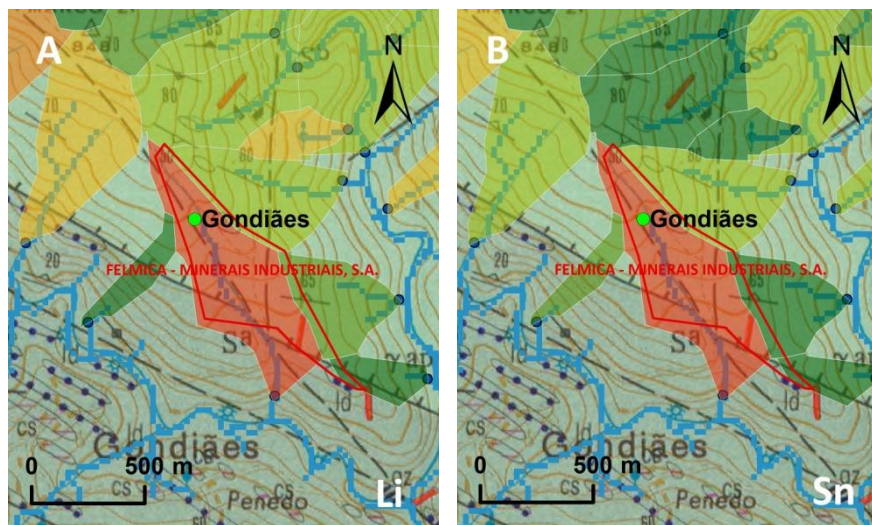


Fig. 37 - Gondiaes aplite-pegmatite vein location on Li-bearing (fig. 36A) and Sn-bearing (fig. 36B) catchment basin maps, using 6C - Cabeceiras de Basto sheet, from the Geological Map of Portugal. The blue lines and blue points represent the waterlines and "SS" points respectively.

4.9. Dias 1 aplite-pegmatite vein

Dias 1 aplite-pegmatite vein had not yet been identified, and was first discovered in the course of this work, moreover it's Li-mineralized, with abundant petalite crystals, where most are about 1 cm wide and 4 cm long. A sample of this vein has been collected (fig. 38).

This aplite-pegmatite vein is embedded in schist with andalusite from Rancho sub-unit, with a N112° foliation, where there is exudation quartz.

Dias 1 is not covered by Li-bearing and Sn-bearing maps, same as Alijó aplite-pegmatite vein, because of the catchment basin where it was located, a main watercourse (Beça river catchment basin). As such, the collected stream sediments are a mixture of other sediments brought by different water streams that flow there.



Fig. 38 – Petalite crystals from Dias 1 aplite-pegmatite vein sample.

4.10. Dias 2 aplite-pegmatite vein

Dias 2 aplite-pegmatite vein was also first discovered while doing field work. Despite of the above referred vein being very weathered, it was still possible to determine that it was Li-mineralized. Some crystals of spodumene and quartz, that seemed to be SQL, were found. It's also probable that this aplite-pegmatite vein has petalite crystals, but due to the degree of the weathering and to the small emerging

area it was impossible to be sure. This vein belongs to Rancho sub-unit metasediments.

Dias 2 is not covered by Li-bearing and Sn-bearing probability maps, since it is outside the stream sediments sampling area.

4.11. Dias 3 aplite-pegmatite vein

Dias 3 aplite-pegmatite vein is a Sn old mine with several galleries, located in the metasediments of Rancho sub-unit. In this vein it was possible to see several millimetric cassiterite needles.

This aplite-pegmatite vein wasn't yet identified as Li-mineralized. However, it has abundant spodumene and quartz crystals (SQI), some of which are about 20 cm long and 10 cm wide. Besides the occurrence of these crystals, Dias 3 is in a catchment basin with high contents in Li and Sn (fig. 39).

Only the most aplitic and weathered parts seem to have been explored, since the more pegmatitic and hard parts seem to have stayed intact.

All the Li-minerals observed at this site seemed to be SQI. As such, this aplite-pegmatite vein, which appears to be now spodumene dominant, could have originally been petalite dominant.

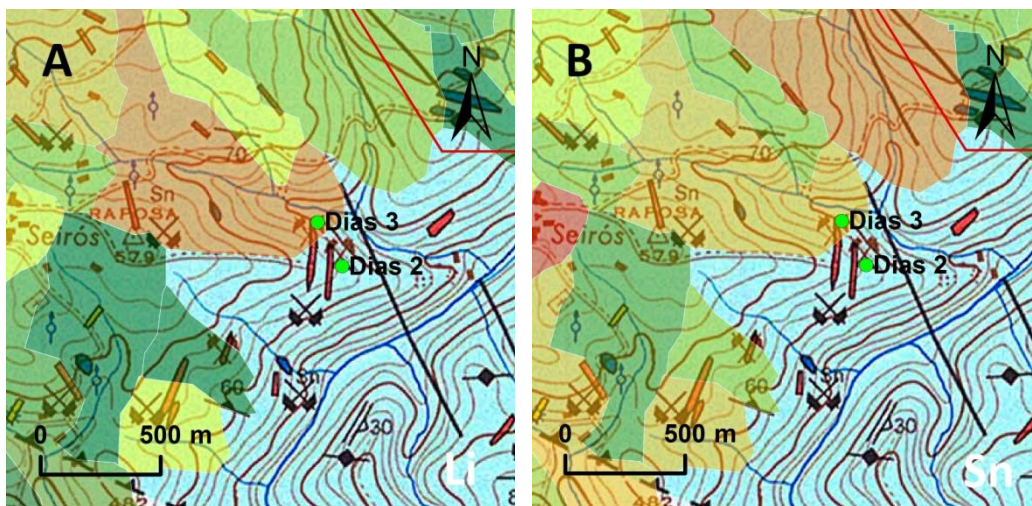


Fig. 39 – Dias 3 aplite-pegmatite vein location on the Li-bearing (fig. 39A) and Sn-bearing (Fig. 39B) catchment basin maps, using the 6D - Vila Pouca de Aguiar sheet, from the Geological Map of Portugal.

Chapter 5 – Petrographic and mineralogical study

5.1. AL56

In the area of the AL56 aplite-pegmatite vein, a sample with several petalite crystals was collected, in which some of them have SQI (fig. 40).

A thin section was made from this sample, containing one of the ends of a petalite crystal that showed the passage of petalite to spodumene + quartz (fig. 41).

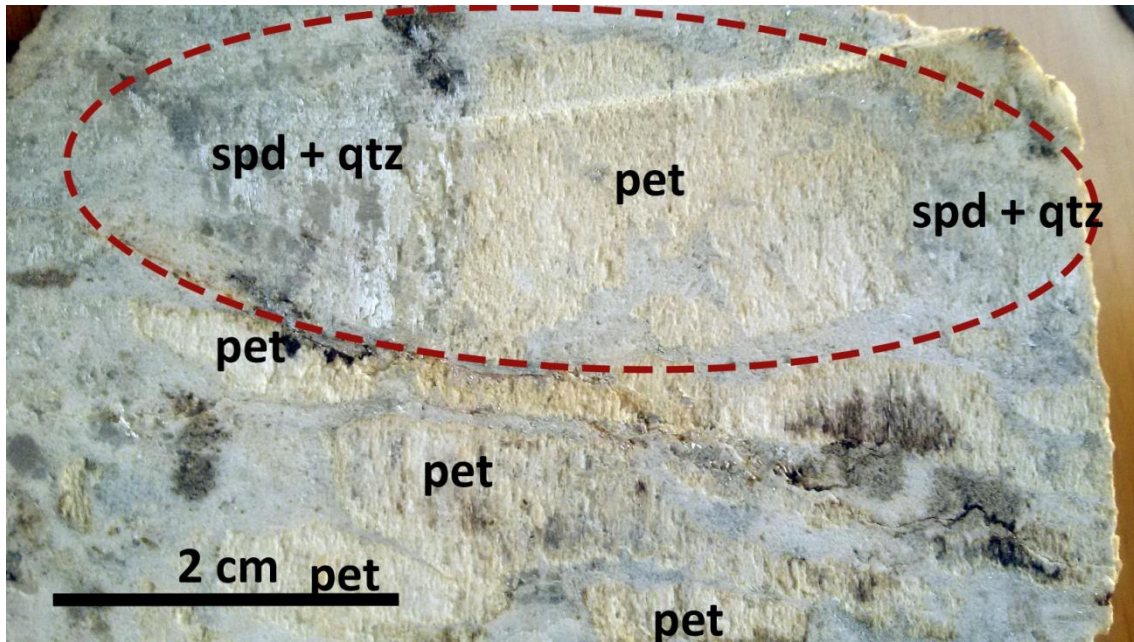


Fig. 40 - Aplite-pegmatite vein sample from AL56 aplite-pegmatite vein area, where it can be seen with the naked eye, a petalite crystal being replaced by spodumene + quartz (SQI). This sample also contains other petalite crystals.

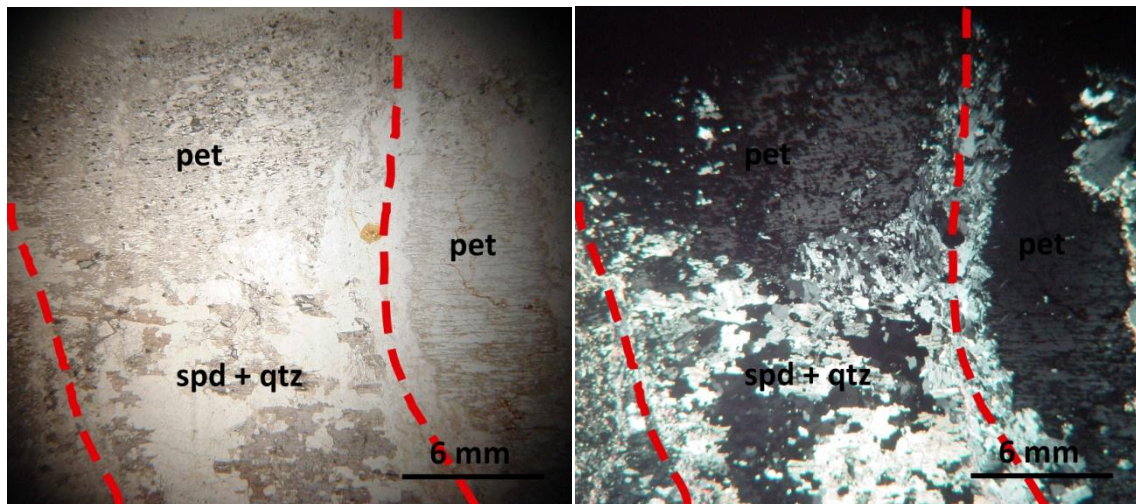


Fig. 41 - Thin section photomicrograph from the sample referred above (fig. 40) where a petalite crystal is being replaced by spodumene + quartz (inside the red dashed line), next to another petalite crystal (on the right side). (A) Plane polarized light. (B) Cross polarized light.

The thin section shows a total of five petalite crystals. In addition to the main crystal where SQI was observed with naked eye, the same occurs on another petalite crystal edge.

About 70% of the thin section is occupied by petalite crystals. The matrix consists of quartz, albite and white mica.

In this thin section the minerals observed were petalite, quartz, spodumene, albite and white mica.

Petalite occasionally has white mica, albite and quartz inclusions. The crystals have irregular borders and it's also common to find white mica crystals along the lateral edges, which often take advantage of the petalite cleavage to grow into them. The petalite crystals do not appear to be deformed.

In one of the petalite crystals it's possible to find an aggregate of small spodumene and quartz crystals along one of the petalite cleavages.

In the thin section, the highest spodumene + quartz (SQI) concentration, belongs to the petalite crystal shown in figure 40 and figure 41, where the replacement can be seen in the ends of the crystal, even with the naked eye. In this thin section, it's possible to see that in the limit of this replacement there is a lateral replacement of petalite to spodumene and quartz (fig. 42A). Spodumene usually grows in the same direction as the petalite cleavage, in other words, with a perpendicular direction to the petalite crystal direction from which it was formed. However, this replacement can also be observed occurring in another petalite crystal, where the spodumene + quartz resemble a symplectite texture (fig. 42B).

One of the other five petalite crystals is very weathered, possessing several small flakes of white mica that appear to be distributed along the cleavages and partitions directions of the old petalite crystal. However, it is still possible to see several petalite relics, alternating with spodumene and quartz relics, that have the same direction of the old petalite cleavage. In this crystal there are also some small albite crystals.

Quartz is one of the main matrix constituents, and can have subgranulation, a deformation indicative. There is also quartz between the spodumene (SQI), which does not appear to be deformed. Quartz also occurs as inclusions, from gotticular to vermicular, within albites and white mica.

Albite is also one of the main constituents of the matrix surrounding the petalite crystals and it's common to show deformation induced twinning, and sometimes bent twinning, which are stress results. These matrix crystals seem to have a tendency to be oriented with the same direction of the bigger petalite crystals. Albite may also occur as petalite crystals inclusions.

The white mica is also one of the matrix constituents and can occur as flakes or needles that can cross each other. Sometimes they also occur along the petalite crystals edges, growing into these crystals through the cleavage planes.

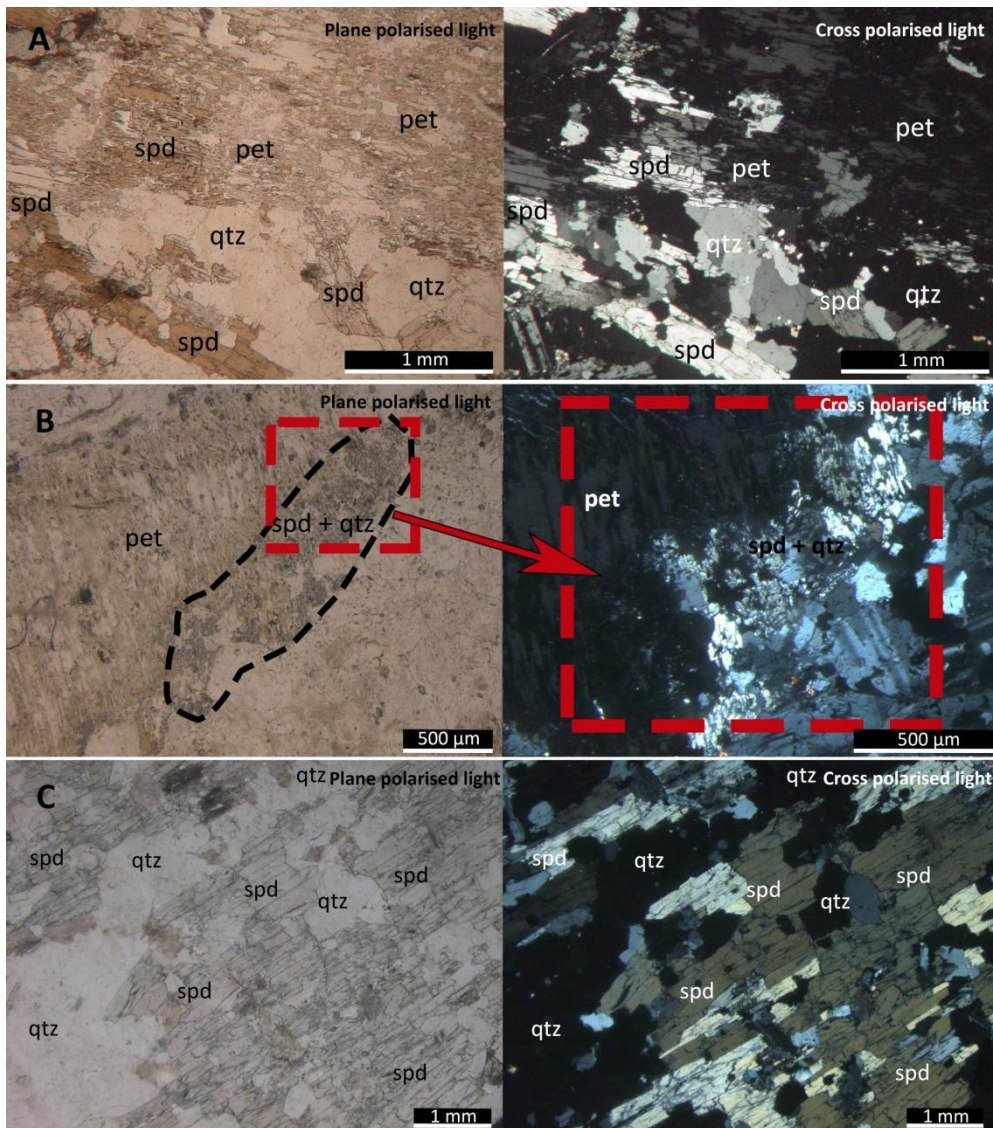


Fig. 42 – Photomicrograph of some of the spodumene aspects from aplite-pegmatite vein in the area of AL56 vein. (A) Lateral replacement of petalite by spodumene and quartz. (B) SQI replacement in another petalite crystal, where the spodumene + quartz resemble a symplectite texture. (C) Close-up on the spodumene and quartz within the main petalite crystal from figure 40 and figure 41.

5.2. CHN3

In general, CHN3 thin sections have an aplitic texture, with some granularity variation. Shear corridors of mylonitic to ultramylonitic textures stand out, showing deformed crystals and ocelli, contoured by the later foliation and with the development of pressure shadows made of small quartz grains (fig.46A). Most ocelli indicate that this is a dextral shear, as observed in the field (fig.43).

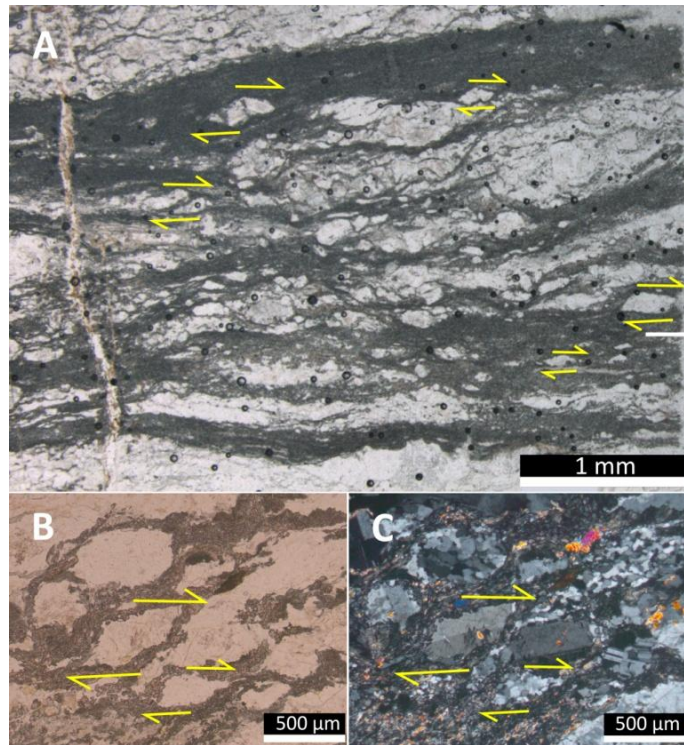


Fig. 43 – Shear corridor from CHN3 aplite-pegmatite vein, with ultramylonitic to mylonitic texture, where most of the ocelli indicate that this is a dextral shear. (B) Ocelli in plane polarized light. (C) Ocelli in cross polarized light. The yellow arrows show the ocelli indicating that this is a dextral shear.

The major mineral phases present are Na-plagioclase (albite), quartz and spodumene and the accessories

include moscovite, petalite, potassium feldspar, ambligonite, cassiterite, apatite and columbo-tantalite. The columbo-tantalite was identified through SEM (Scanning Electron Microscope) at CEMUP (Materials Center of the University of Porto).

Albite is very abundant and is uniformly distributed along the thin sections. It's common to show deformation induced twinning and bent twinning, resulting from stress (fig. 46B). The crystals don't have a main direction and contain some apatite, moscovite inclusions, and more commonly drop-like and vermicular (worm-like) inclusions (fig. 46C). The albite crystals may be of a very small size, forming what seems a mosaic, together with recrystallized quartz (fig. 46D). Albite can also occur within the shear corridors as ocelli.

Quartz resulting from dynamic recrystallization is very common, forming a texture of small, irregular crystals with a uniform size (fig. 46E). However, larger quartz grains also occur, some with undulose extinction and others with deformation lamellae. These phenomena correspond to mechanisms of deformation resulted from stress

where dynamic recrystallization is the final stage of a recovery process. Quartz may also contain inclusions of albite, moscovite, and apatite.

Spodumene isn't uniformly distributed along the thin sections, being usually in localized areas, forming aggregates. It occurs with different sizes from large euhedral crystals of about 500 μm to 2 mm, that are oriented and have quartz grain intergrowths (fig. 45A and fig. 45B), to small spodumene and quartz aggregates, with very irregular shapes, forming alignments along the thin sections (fig. 45C and fig. 45D). The larger spodumene and quartz aggregates have an elongated shape and, occasionally, on the edges of these agglomerates, the spodumene may have a symplectite texture. This intercalation of spodumene and quartz resembles SQI. In these thin sections there are also posterior, small and prismatic-like crystals, that are associated with the shear zones (fig. 45E). In SEM (Scanning Electron Microscope) these were found to be made of alternate spodumene and quartz.

Muscovite, despite being relatively scarce, is the most abundant accessory mineral. The larger crystals usually have a size between 500 μm - 1mm. It's common for these to be curved (fig. 46F), a deformation result, and may contain quartz inclusions. There are many small moscovite flakes, with irregular borders, in intergranular spaces. Moscovite can also occur as inclusions in albite and quartz crystals.

Petalite is one of the accessory minerals of this thin sections and it's possible to find some places with petalite being replaced by spodumene + quartz. This type of replacement, has already been seen in the petalite crystals of the aplite-pegmatite vein in AL56 area, appears to start by the edges of the petalite crystals and the spodumene appears to grow perpendicularly to the former petalite crystal (fig. 41).

K-feldspar was occasionally found showing the typical cross-hatched twin pattern of microcline. However, other K-feldspars may occur with simple twinning, making them hard to distinguish from the abundant albite crystals (fig. 46G).

Amblygonite is also a bit rare and the largest observed crystals are about 800 μm . It's common to exhibit the typical polysynthetic twinning. They can also be found within the shear corridors as ocelli (fig. 46A).

Cassiterite is scarce, has pleochroism and is fractured. The largest observed crystals are about 200 μm . However, within the shear corridor there is also smaller, deformed cassiterite, oriented in the direction of the fabric and without fractures, which

indicates that these crystals, just like those of amblygonite, are older compared with the shear corridors. The cassiterite can exhibit simple twinning.

Theoretically, the replacement of petalite to spodumene + quartz would result in 56% spodumene and 44% quartz.

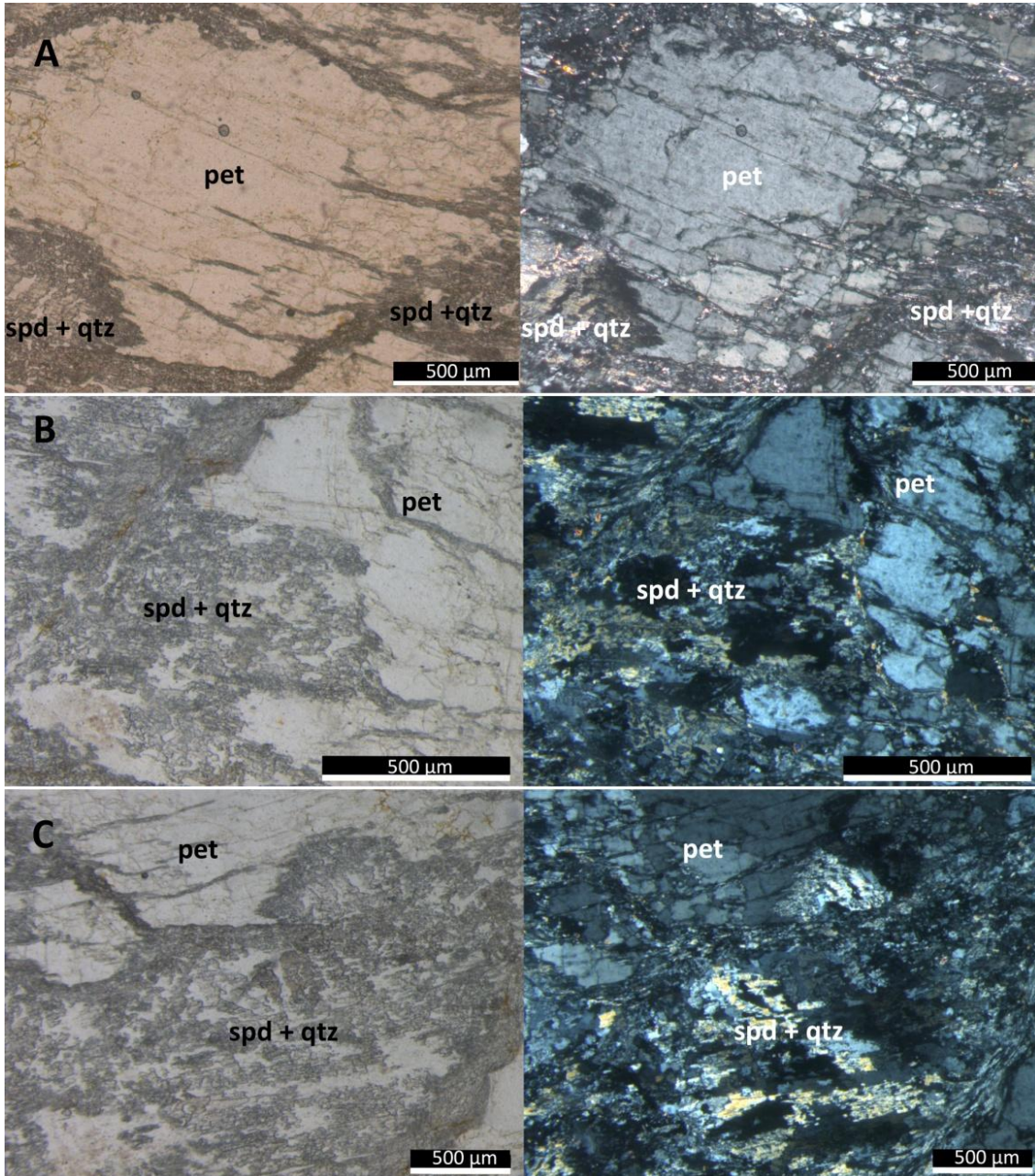


Fig. 44 - Photomicrograph of petalite being replaced by spodumene and quartz (SQI) from CHN3 aplite-pegmatite vein.

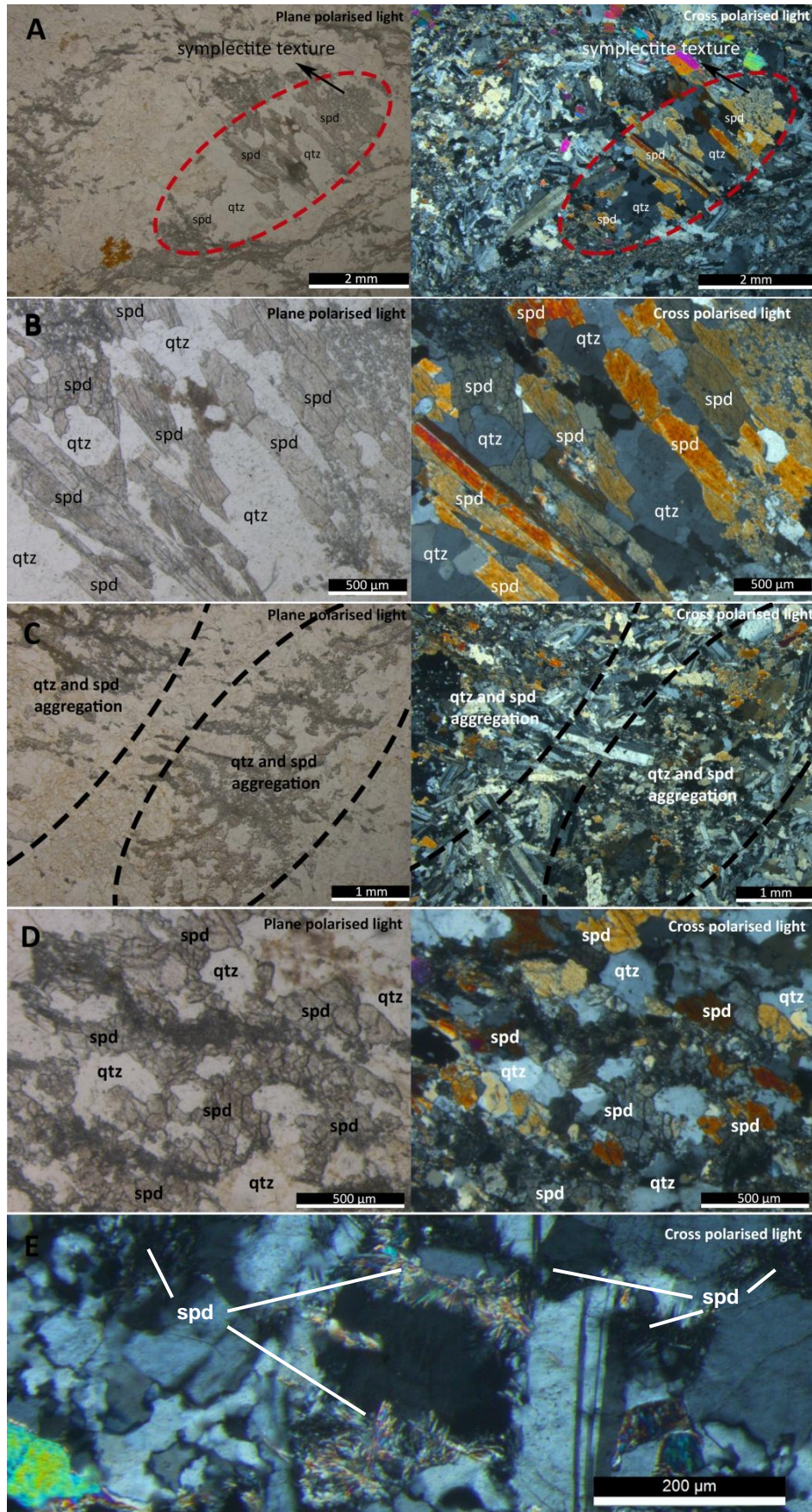


Fig. 45– Photomicrograph of some features of spodumene from CHN3 aplite-pegmatite vein. (A) Largest spodumene and quartz crystals in an elongated aggregate, where it's possible to see the symplectite texture at one end. (B) Close-up of fig. 41A. (C) Small spodumene and quartz crystals in a elongated aggregate. (D) Close-up of Fig. 41C. (E) Small spodumene crystals posterior to the shear.

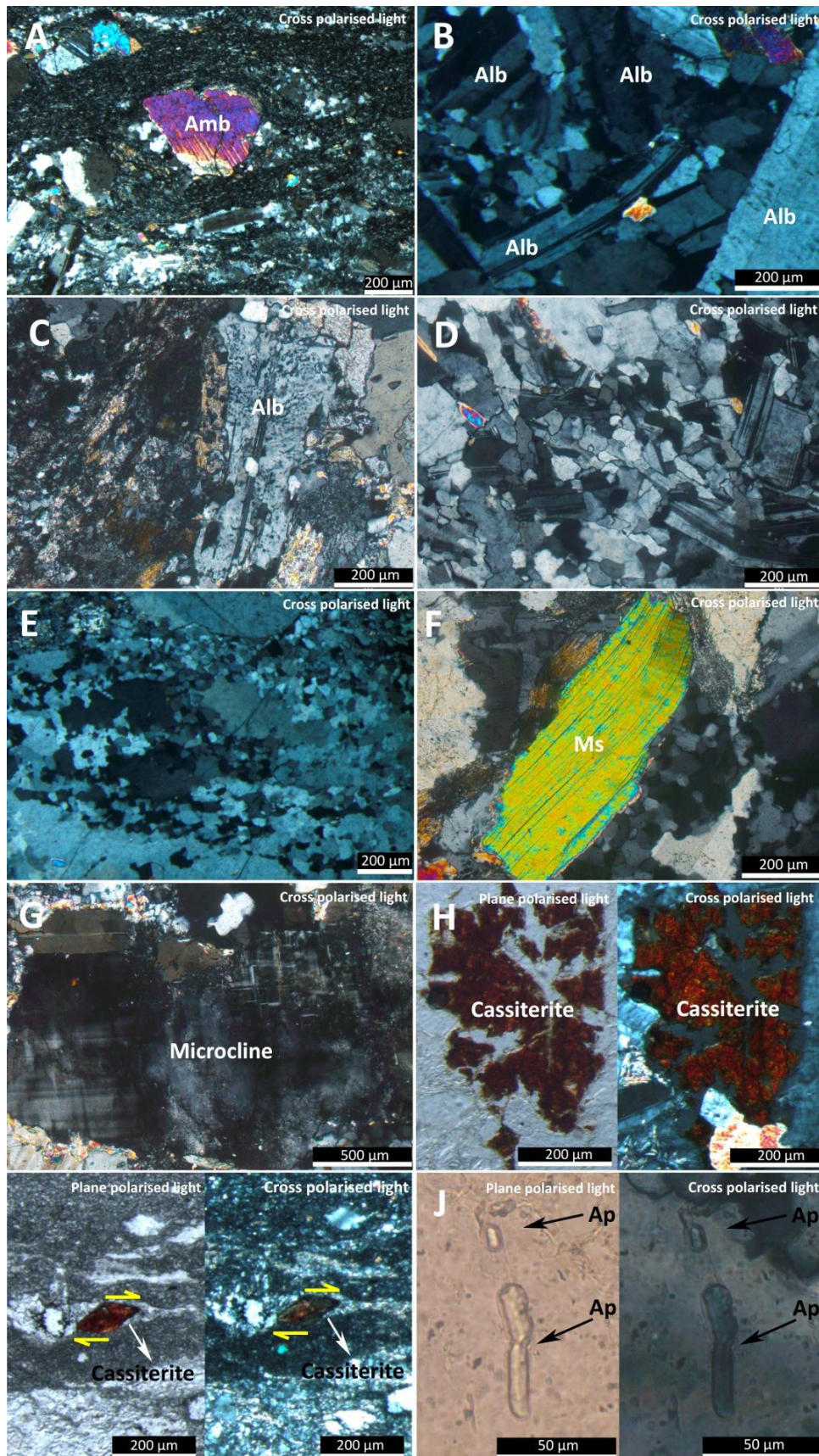


Fig. 46 – Photomicrograph with some features of the CHN3 thin section. (A) Ambligonite ocelli with pressure shadows. (B) Albites with deformation induced twinning and bent twinning. (C) Vermicular quartz inclusions on an albite crystal. (D) Small crystals of quartz and albite forming what seems to be a mosaic. (E) Quartz resulting from dynamic recrystallization. (F) Deformed muscovite. (G) Microcline with the typical cross-hatched twin pattern (H) Fractured cassiterite. (I) Deformed cassiterite within a shear corridor. (J) Apatite inclusion on quartz.

Chapter 6 – Discussion and conclusions

The method of using the Li-bearing and Sn-bearing catchment basins maps to find Li-mineralized veins during field work showed good potential. It allows to cover large areas by collecting and analyzing stream sediments and defining potential mineralized areas. Therefore, it seems to be a good prospecting method and can be applied to other areas of interest.

Taking in consideration, that the aplite-pegmatite veins from old Sn mining works can also be seen as potential zones to find petalite, we have new exploration targets to obtain lithium. The referred Dias 3, Gondíães and Lousas aplite-pegmatite veins are some examples.

In the figures 47A and 47B, the Li-bearing and Sn-bearing catchment basin maps show another example of an old Sn mining work in an aplite-pegmatite vein located in a potentially mineralized area with high probability of containing petalite mineralization (has high Li- and Sn-contents). This one belongs to a recent example of mineral exploration for lithium ores, where a drill campaign was carried out (Dakota Minerals, 2016a).

Romano old Sn mine was the first place where a borehole was made within the scope of the Sepeda Lithium Project (fig. 47). According to Dakota Minerals (2016b), the results show that the ore contains mainly petalite, with some associated spodumene, and that the petalite has high Li-contents. Therefore, the results obtained through my study are coincident with those from the borehole, confirming that the main Li-mineral from Romano aplite-pegmatite vein is petalite.

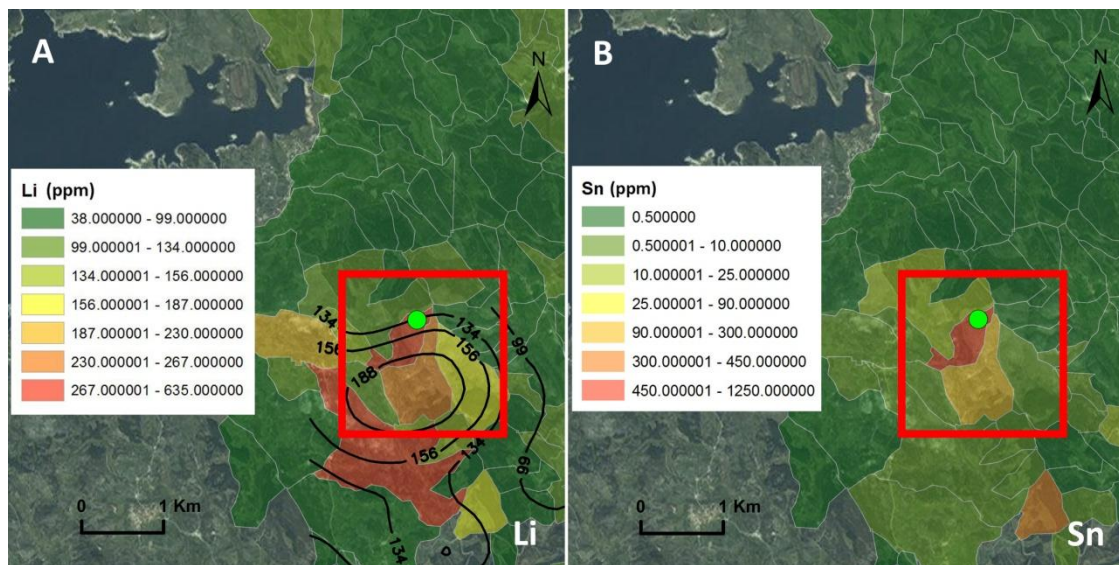


Fig. 47 – Location of Romano old Sn mine (green point) in the Li-bearing (fig.47A) and Sn-bearing (fig.47B) catchment basin maps. The coordinates of this aplite-pegmatite vein are 41°44'14.592" W 7° 43'43.591"W. The red outline represents the planned drill area by Dakota Minerals. In Pires (2005) this zone had already been identified as having high Li-contents, as represented by the black counter lines in the fig.47A. The catchment basins create now smaller and more precise Li-rich areas.

Dakota Minerals also states that many of the pegmatites in that area (Sepeda Lithium Project) do not outcrop and are only visible through old mining works. This statement, also confirms that old Sn mines should be seen has potential places do find Li-minerals, even more if it's an area with high Li-content.

As for the aplite-pegmatite veins genetic model, it hasn't been found within the aplite-pegmatite population any apparent spatial zonation with the local granites. Therefore, the model defended by Deveaud et al. (2014) of a low melting rate of crustal material with successive injections of different melts, favored by regional shear-zones, seems to be a good theory.

With this study, it can also be concluded that the occurrence of SQI in the Barroso-Alvão aplite-pegmatite field is a more common occurrence than previously thought. Therefore, if we are seeing a dominant spodumene vein it must be taken into account that this spodumene could be SQI.

For example, it was assumed that the aplite-pegmatite vein in AL56 area, within the Imerys Ceramics Portugal, S.A. mining concession, was a spodumene vein because of having dominant spodumene. However, this would initially be a dominant petalite vein since all the crystals rich in spodumene seem to be SQI. The same is verified in the Dias 3 aplite-pegmatite vein, in which this isochemical replacement of petalite by spodumene and quartz (SQI) was observed in countless crystals localized in an old Sn mining work. SQI was also observed in Lousas aplite-pegmatite vein, where the major Li-phase is petalite. Spodumene crystals, that probably are SQI, also occur at the ends of the Gondiaes aplite-pegmatite vein.

CHN3 aplite-pegmatite vein also belongs to this group of prior petalite when compared to spodumene. In addition to the petalite found in the field and in the thin sections, it was also observed its replacement to SQI. Finally, there is also cassiterite, prior to the shear-zones that is commonly associated with petalite veins.

Finally, it seems that shear-zones cutting Li-rich aplite-pegmatite veins can generate a recrystallization of new small crystals that are constituted by spodumene and quartz, like what was found in the CHN3 aplite-pegmatite vein.

References

- Amarante, M. M., Botelho de Sousa, A. and Machado Leite, M. (1999). *Processing a spodumene ore to obtain lithium concentrates for addition to glass and ceramics bodies*. IGM - Geological and Mining Institute (now named LNEG - National Laboratory of Energy and Geology). Minerals Engineering, Vol. 12. Nº. 4. pp. 433-436. Portugal.
- Cerný, P. and Ercit, T. (2005). *The classification of granitic pegmatites revisited*. The Canadian Mineralogist Vol.43. pp 2005-2026
- Charoy, B., Lhote, F. and Dusausoy, Y. and Noronha, F. (1992). *The Crystal Chemistry of Spodumene in Some Granitic Aplite-Pegmatite of Northern Portugal*. Canadian Mineralogist. Vol.30, pp. 639-651.
- Charoy, B. and Noronha, F. (1988). *A espodumena como fase litinífera de aplitopegmatitos da região de Covas de Barroso (Norte de Portugal)*. Resumos da X Reunião sobre a Geologia do Oeste Peninsular (Coimbra-Salamanca).
- Charoy, B., Noronha, F. and Lima A. (2001). *Spodumene-Petalite-Eucryptite: mutual relationships and alteration style in pegmatite-aplite dykes from Northern Portugal*. Canadian Mineralogist. Vol. 39, pp. 729-746.
- Deveaud, S., Silva, D., Gumiaux, C., Gloaguen, E., Branquet, Y., Lima, A., Villaros, A., Guillou-Frottier, L. and Melleton J. (2014). *Which parameters control the Variscan pegmatite field-scale organization?*
- Dória, A., Charoy, B. and Noronha, F. (1989). *Fluid inclusion studies in spodumene bearing pegmatite-aplite dykes of Covas de Barroso, Northern Portugal*. ECROFI X. Program Abstr. Londres. pp 25.
- Farinha, J. (1998). *Prospecção de Jazidas Litiníferas e de Metais Associados entre as Serras do Barroso e Alvão. (Alto Tâmega)*. IGM - Geological and Mining Institute (now named LNEG - National Laboratory of Energy and Geology). Portugal
- Farinha, J. (2012). *Cartografia Geológica de Detalhe e Levantamento Topográfico Expedido do Filão Aplitopegmatítico N°103: Dornelas - Boticas*. IGM - Geological and Mining Institute (now named LNEG - National Laboratory of Energy and Geology) - Departamento de Prospecção de Minérios Metálicos. Coimbra.
- Farinha, J. and Lima, A. (2000). *Estudo dos filões aplitopegmatíticos litiníferos da Região do Barroso-Alvão (Norte de Portugal)* Estudos, Notas e Trabalhos. Tomo

42. IGM - Geological and Mining Institute (now named LNEG - National Laboratory of Energy and Geology). Lisboa. pp. 3 – 49.
- Holtz, F. (1987). *Étude structurale, métamorphique et géochimique des granitoides hercyniens et de leur encaissant dans la région de Montalegre (Trás-os-Montes, Nord Portugal)*. Ph. D. thesis. Nancy University. 223 pp.
- Lima, A. (2000). *Estrutura, Mineralogia e Génese dos Filões Aplitepegmatíticos com Espodumena da Região do Barroso-Alvão*. Ph. D. thesis in Sciences (Geologia). Faculty of Sciences of University of Porto. Porto.
- Lima, A. and Noronha, F. (2006). *Da génese à aplicação tecnológica dos aplitepegmatitos litiníferos da Região do Barroso-Alvão e de Almendra*. VII Congresso Nacional de Geologia – Resumos alargados. Évora University. Vol 3. pp. 1183 - 1184.
- Lima, A., Noronha, F. and Bobos, I. (2007). *Hydrothermal Alteration Process of the Lithium Bearing Aplite-Pegmatite Veins from the Barroso-Alvão Field, Portugal*. Memórias N.º 9 - Granitic Pegmatites: The State of the Art - Field Trip Guidebook. Editado por Alexandre Lima e Encarnación Roda Robles. Porto.
- Lima, A., Martins T., Vieira R. and Noronha F. (2011). *Campo aplitepegmatítico litinífero do Barroso-Alvão. Os seus diferentes minerais de lítio e sua melhor aplicação futura*. Mini-fórum Cyted-Iberoeka - Valorização de Pegmatitos Litiníferos. Colaboração: DGEG-Direcção Geral de Energia e Geologia; LNEG-Laboratório Nacional de Energia e Geologia. Apoio: CYTED-Ciencia y Tecnología para el Desarrollo; LNEG-Laboratório Nacional de Energia e Geologia. Lisboa.
- Kogel, J., Trivedi, N., Barker, J. and Krukowski, S. (2006). *Industrial Mineral & Rocks*. 7ª edição. Society for Mining, Metallurgy, and Exploration, Inc. Colorado, Estados Unidos da América (USA). 601 pp.
- Martins, T. (2009). Multidisciplinary study of pegmatites and associated Li and Sn-Nb-Ta mineralisation from the Barroso-Alvão region. Ph. D. thesis in Geology (Geologia). Faculty of Sciences of University of Porto. Porto.
- Martins, T. and Lima A. (2011). *Pegmatites from Barroso-Alvão, Northern Portugal: anatomy, mineralogy and mineral geochemistry*. Cadernos Lab. Xeolóxico de Laxe. Corunha. Vol. 36. pp. 177 - 206.

- Martins, T., Lima, A. and Noronha, F. (2007). *Locality No. 1 - An overview of the Barroso-Alvão Aplite-Pegmatite Field*. Memórias N° 9 - Granitic Pegmatites: The State of the Art - Field Trip Guidebook. Edited by Alexandre Lima e Encarnación Roda Robles. Porto.
- Martins, T., Lima, A., Vieira, R., Noronha, F. and Dinis Machado, J. (2006). *Aplitopegmatitos litiníferos, um exemplo de Recursos Geológicos no Município de Ribeira de Pena*, VII Congresso Nacional de Geologia – Resumos alargados, University de Évora. Évora. Vol. 3 . pp. 1035 – 1036.
- Moura, A. and Velho, J. (2012). *Recursos Geológicos de Portugal*. Palimage. Coimbra. pp. 245 – 250.
- Noronha, F. and Charoy, B. (1991). *Pegmatitos graníticos com elementos raros da região de Barroso (Norte de Portugal)*. Resumos do I Congresso de Geoquímica dos Países de Língua Portuguesa. S. Paulo University, 1, pp 276-279.
- Noronha, F., Ribeiro, M. A., Almeida, A., Dória, A., Guedes, A., Lima, A., Martins, H. C., Sant’Ovaia, H., Nogueira, P., Martins, T., Ramos, R. and Vieira, R. (2006). *Jazigos filonianos hidrotermais e aplitopegmatíticos espacialmente associados a granitos (Norte de Portugal)*. Geologia de Portugal no Contexto da Ibéria. Évora University. Évora. pp. 123 – 135.
- Pacheco, F., Moreiras, P. and Matias, R. (2006). *Caracterização Industrial do Filão Aplito-pegmatítico com Espodumena de Alijó (Ribeira de Pena, Norte de Portugal)*. VII Congresso Nacional de Geologia – Resumos alargados. Évora University. Évora. Vol. 3. pp. 1048.
- Pires, M. (1995). *Prospecção Geológica e Geoquímica. Relatório interno da Prospecção de Jazidas Litiníferas e de Metais Associados entre as Serras de Barroso e Alvão – Ribeira de Pena*. IGM - Geological and Mining Institute (now named LNEG - National Laboratory of Energy and Geology). Lisboa.
- Reichl, C., Schatz, M., and Zsak, G. (2016). *World Mining Data - Minerals Production*. 31º Volume. International Organizing Committee for the World Mining Congresses. Viana.
- Ribeiro, M. A. (1998). *Estudo litogeoquímico das formações metassedimentares encaixantes de mineralizações em Trás-os-Montes Ocidental: Implicações*

metalogénicas. Ph. D. thesis in Geology. Faculty of Sciences of University of Porto. Porto.

Sant' Ovaia, H., Ribeiro, M.A., Martins, H. C. B. and Noronha, F. (2011). *Notícia explicativa da Carta geológica de Portugal na escala 1:50000 - Folha 6D – Vila Pouca de Aguiar*. LNEG - National Laboratory of Energy and Geology. Lisboa.

Silva, D. (2014). *Spatial analysis applied to the Barroso-Alvão rare-elements pegmatite field (Northern Portugal)*. Master's thesis in Geology. Faculty of Sciences of University of Porto. Porto.

Sitando, O. and Crouse, P.L. (2011). *Processing of a Zimbabwean petalite to obtain lithium carbonate*. International Journal of Mineral Processing.

Viegas, H., Martins, L. and Oliveira, D. (2012) *Alguns aspectos da geoestratégia global do lítio. O caso de Portugal*. Geonovas, n.º 25. pp. 19-25.

Webber, K. (2007). *Crystallization Dynamics*. Granitic Pegmatites: the state of the art. International Symposium. 6º. Porto. Portugal.

Webber, K., Simmons, W. and Falster A. (2005). *Rapid Conductive Cooling of Sheet-Like Pegmatites*.

List of websites consulted

Australian Government – Geoscience Australia (2013). *Lithium*. Available at Australian atlas of minerals resources, mines & processing centres website:
<http://www.australianminesatlas.gov.au/aimr/commodity/lithium.html> (retrieved: 17/09/2016)

Bryner, M., Clarke, G., Jansen, A., Patel, A. and Spotnitz R. (2013). *Lithium-Ion Batteries*. American Institute of Chemical Engineers (AIChE). New York. Available at: https://www.aiche.org/sites/default/files/cep/20131033-64_r.pdf (retrieved: 18/09/2016)

Dakota Minerals (2016). *Strategic Lithium Acquisition in Portugal* (Announcement). Available at:

https://www.google.pt/url?sa=t&rct=j&q=&esrc=s&source=web&cd=1&ved=0ahUKewifk--u9pvPAhWHCsAKHXeICTQQFggBMAA&url=http%3A%2F%2Fwww.dakotaminerals.com.au%2Findex.php%2Fasx-announcements%2F2016%2Fdownload-file%3Fpath%3D1559741.pdf&usg=AFQjCNFCi0vSS5YRVV_A2Z7JHx0-SrM5Qg&sig2=pWFy_pS6MPP1uelms3DyZw&bvm=bv.133178914,d.ZGg&cad=rja (retrieved: 15/09/2016)

Dakota Minerals (2016a). *Drilling Commences at Sepeda Lithium Project, Portugal* (Announcement). Available at Investor Insight website:
<http://www.asx.com.au/asxpdf/20160830/pdf/439rynq0jimpf50.pdf> (retrieved: 22/09/2016)

Dakota Minerals (2016b). *Phase two Drilling brought forward after Encouraging Initial Drill Results from Sepeda Lithium Project – Portugal*. (Announcement). Available at:
<http://www.dakotaminerals.com.au/index.php/asx-announcements/2016/download-file?path=1602965.pdf> (Retrieved: 10/10/2016)

Dakota Minerals (2016c). *Major European Lithium Discovery Confirmed - Sepeda Project, Portugal* (Announcement). Available at:
<http://www.dakotaminerals.com.au/index.php/asx-announcements/2016/download-file?path=1614613.pdf> (Data de consulta: 8/11/2016)

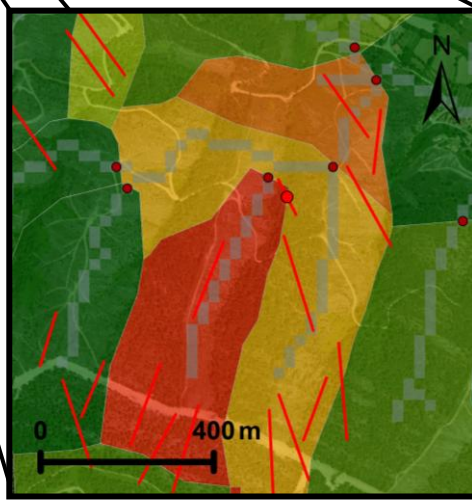
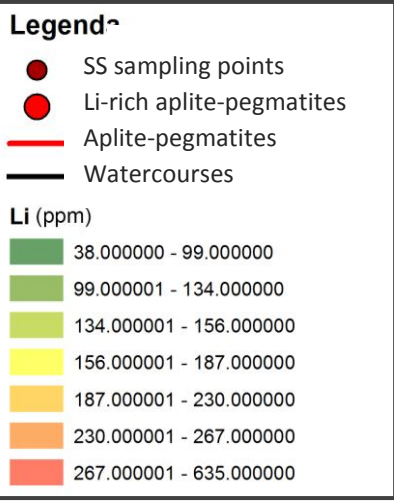
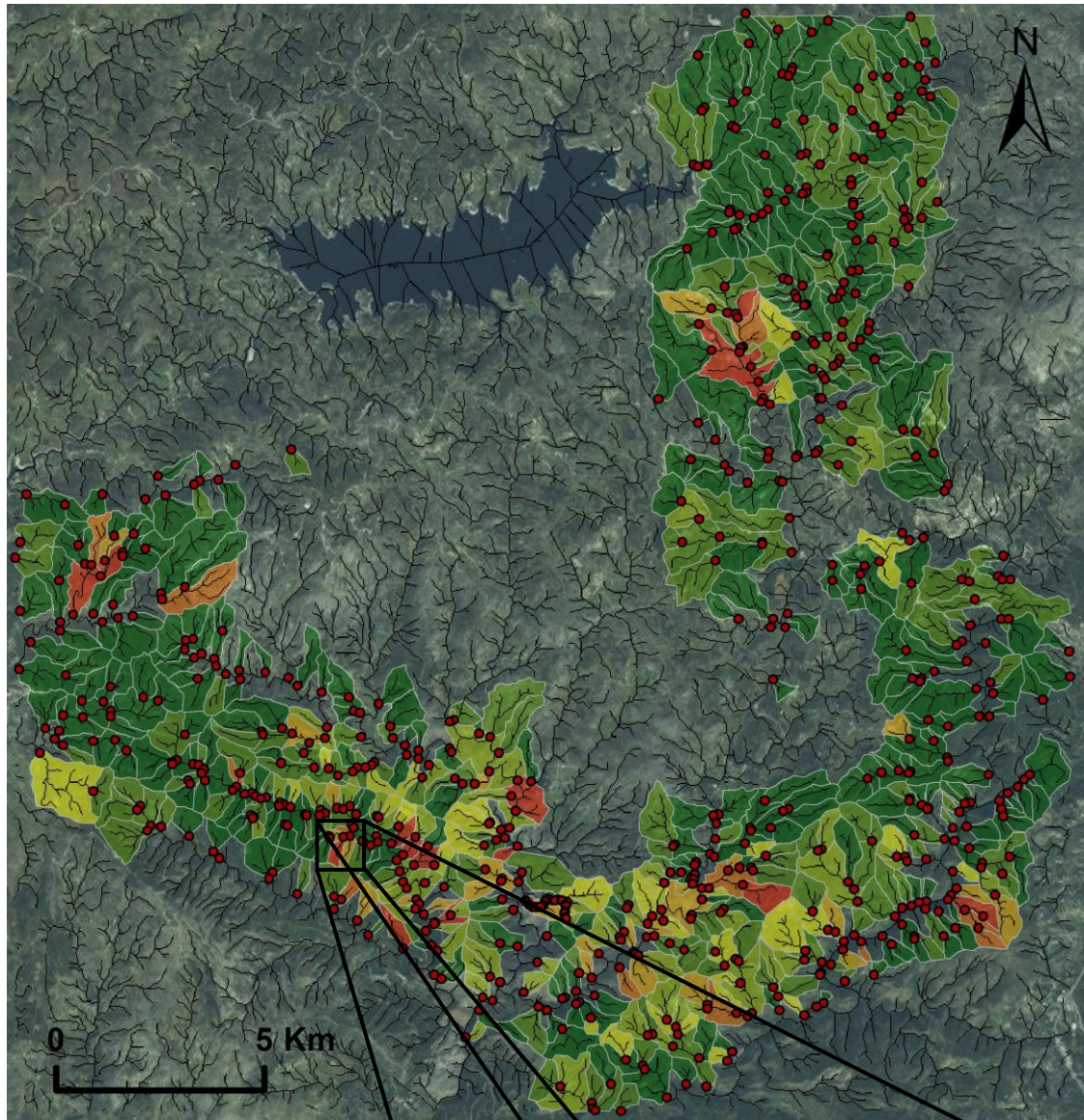
European Comission (2014). *Report on critical raw materials for the EU – Non-critical raw materials profiles*. Available at European Comission website:
<http://ec.europa.eu/DocsRoom/documents/7422/attachments/1/translations> (retrieved: 16/09/2016)

European Comission (2014a). *Annexes to the report on critical raw materials for the EU*. Available at European Comission website:
<http://ec.europa.eu/DocsRoom/documents/10011/attachments/1/translations> (retrieved: 15/09/2016)

Annexes

Annex 1

Illustration of Li-bearing catchment basins final result, mentioned in Chapter 3: "bacias_hidro_final_cortadas".



Annex 2

Geographic coordinates of the aplite-pegmatite veins visited during the field work

Li-mineralized aplite-pegmatite veins	Geographic coordinates (Datum WGS 84)	
	Latitude	Longitude
N312-1 aplite-pegmatite vein	41°36'33.45"N	7°43'13.48"W
N312-2 aplite-pegmatite vein	41°36'25.84"N	7°43'25.08"W
CHN3 aplite-pegmatite vein	41°35'45.84"N	7°47'16.85"W
Alijó aplite-pegmatite vein	41°36'29.74"N	7°45'11.86"W
Pinheiro aplite-pegmatite vein	41°36'15.67"N	7°45'46.38"W
Vila Grande Aplite-pegmatite vein	41°38'15.42"N	7°51'3.30"W
Lousas aplite-pegmatite vein	41°37'20.44"N	7°49'47.59"W
AL56 aplite-pegmatite vein	41°37'51.67"N	7°48'41.15"W
Gondiães aplite-pegmatite vein	41°36'12.42"N	7°50'01.48"W
Dias 1 aplite-pegmatite vein	41°35'14.74"N	7°46'27.40"W
Dias 2 aplite-pegmatite vein	41°34'44.90"N	7°43'49.87"W
Dias 3 aplite-pegmatite vein	41°34'50.84"N	7°43'53.97"W

Geographic coordinates of old Sn mining works visited during the field work

Id	Geographic coordinates (Datum WGS 84)	
	Latitude	Longitude
1	41°35'57.54"N	7°44'3.41"W
2	41°36'8.40"N	7°47'10.91"W
3	41°35'22.41"N	7°45'0.90"W
4	41°35'19.00"N	7°45'0.00"W